

AD\_\_\_\_\_

Award Number: W81XWH-04-1-0219

TITLE: Microtubule-Targeting Therapy for Prostate Cancer

PRINCIPAL INVESTIGATOR: George F. Atweh, M.D.

CONTRACTING ORGANIZATION: Mount Sinai School of Medicine  
New York, NY 10029-6574

REPORT DATE: February 2007

TYPE OF REPORT: Final

PREPARED FOR: U.S. Army Medical Research and Materiel Command  
Fort Detrick, Maryland 21702-5012

DISTRIBUTION STATEMENT: Approved for Public Release;  
Distribution Unlimited

The views, opinions and/or findings contained in this report are those of the author(s) and should not be construed as an official Department of the Army position, policy or decision unless so designated by other documentation.

REPORT DOCUMENTATION PAGE				Form Approved OMB No. 0704-0188	
Public reporting burden for this collection of information is estimated to average 1 hour per response, including the time for reviewing instructions, searching existing data sources, gathering and maintaining the data needed, and completing and reviewing this collection of information. Send comments regarding this burden estimate or any other aspect of this collection of information, including suggestions for reducing this burden to Department of Defense, Washington Headquarters Services, Directorate for Information Operations and Reports (0704-0188), 1215 Jefferson Davis Highway, Suite 1204, Arlington, VA 22202-4302. Respondents should be aware that notwithstanding any other provision of law, no person shall be subject to any penalty for failing to comply with a collection of information if it does not display a currently valid OMB control number. <b>PLEASE DO NOT RETURN YOUR FORM TO THE ABOVE ADDRESS.</b>					
1. REPORT DATE (DD-MM-YYYY) 01-02-2007		2. REPORT TYPE Final		3. DATES COVERED (From - To) 16 Jan 04 – 15 Jan 07	
4. TITLE AND SUBTITLE Microtubule-Targeting Therapy for Prostate Cancer				5a. CONTRACT NUMBER	
				5b. GRANT NUMBER W81XWH-04-1-0219	
				5c. PROGRAM ELEMENT NUMBER	
6. AUTHOR(S) George F. Atweh, M.D.  E-Mail: <a href="mailto:george.atweh@mssm.edu">george.atweh@mssm.edu</a>				5d. PROJECT NUMBER	
				5e. TASK NUMBER	
				5f. WORK UNIT NUMBER	
7. PERFORMING ORGANIZATION NAME(S) AND ADDRESS(ES)  Mount Sinai School of Medicine New York, NY 10029-6574				8. PERFORMING ORGANIZATION REPORT NUMBER	
9. SPONSORING / MONITORING AGENCY NAME(S) AND ADDRESS(ES) U.S. Army Medical Research and Materiel Command Fort Detrick, Maryland 21702-5012				10. SPONSOR/MONITOR'S ACRONYM(S)	
				11. SPONSOR/MONITOR'S REPORT NUMBER(S)	
12. DISTRIBUTION / AVAILABILITY STATEMENT Approved for Public Release; Distribution Unlimited					
13. SUPPLEMENTARY NOTES-Original contains colored plates: ALL DTIC reproductions will be in black and white.					
14. ABSTRACT: 1. Misry, SJ, Bank A, Atweh, GF. Cell cycle inhibition therapy: Stathmin as a potential therapeutic target in prosProceedings of the American Association of Cancer Research, Abstract #3039, 2004. 2. Mistry, SJ, Perez Y, Atweh, GF. Therapeutic interactions of anti-stathmin therapy with chemotherapeutic agents incancer. Proceedings of the American Association of Cancer Research, Abstract #4940, 2005. 3. Mistry, SJ, Atweh, GF. Microtubule targeting therapy in vivo. Proceedings of the American Association of CanceAbstract # 524, 2006.					
15. SUBJECT TERMS Cell biology, integrins, KAI1/CD82, tetraspanins, metastasis, androgen, signal transduction, 3-D culture					
16. SECURITY CLASSIFICATION OF:			17. LIMITATION OF ABSTRACT	18. NUMBER OF PAGES	19a. NAME OF RESPONSIBLE PERSON
a. REPORT	b. ABSTRACT	c. THIS PAGE			USAMRMC
U	U	U	UU	30	19b. TELEPHONE NUMBER (include area code)

## Table of Contents

	<u>Page</u>
Introduction.....	1
Body.....	1-7
Key Research Accomplishments.....	7
Reportable Outcomes.....	7 -8
Conclusion.....	8
References.....	8-9
Appendices.....	

## A. INTRODUCTION

Prostate cancer is the most frequently diagnosed malignancy and the second leading cause of cancer-related deaths in men in the U.S. In the early stage of the disease, the treatments of choice are extensive surgery and/or radiation therapy. Although both treatment modalities are effective, they are associated with significant morbidity and mortality. When local therapies for prostate cancer fail and the disease progresses, systemic androgen ablation therapy, with or without chemotherapy, can frequently lead to tumor regression. However, the disease inevitably progresses to an androgen-independent state that is resistant to hormonal therapy and chemotherapy. Thus, the development of alternative therapeutic strategies for prostate cancer in the early and the late stages remains a high-priority.

The focus of our research is to develop a novel therapeutic strategy for the treatment of prostate cancer that targets the microtubules that make up the mitotic spindle. Stathmin is a founding member of a family of microtubule-destabilizing proteins that play a critical role in the regulation of mitosis. This protein is expressed at high levels in a wide variety of human malignancies, including prostate carcinoma. When biopsy specimens from human prostate cancers were immunostained with an anti-stathmin antibody, immunoreactivity was seen in poorly differentiated tumors but not in hyperplastic prostate or in highly differentiated prostate cancer. More importantly, the level of expression of stathmin was shown to correlate with the malignant behavior of prostate cancer cells. As a matter of fact, it was proposed that the level of expression of stathmin may serve as an important prognostic marker in prostate cancer. Thus, stathmin provides an attractive target for prostate cancer therapy. Moreover, the localized aspect of the disease in its early stages and its responsiveness to local therapy makes prostate cancer an attractive model for the development of a stathmin-based local therapy that might avoid the morbidity and mortality of extensive surgery and radiation therapy.

## B. BODY

In our grant application entitled “Microtubule targeting therapy for prostate cancer”, we proposed 3 specific aims: (1) Investigate the effects of stathmin inhibition by adenoviral vectors *in vitro* in prostate cancer; (2) Investigate the effects of stathmin inhibition by adenoviral vectors *in vivo* in mouse models of human prostate cancer; (3) Investigate the effects of the combination of stathmin inhibition and taxol on tumorigenesis in *in vitro* and *in vivo* models of human prostate cancer. In this section, we will briefly summarize the experiments that were done to achieve the above specific goals.

**1. Biological effects of ribozyme-carrying adenoviruses that target stathmin mRNA in human prostate cancer cells:** A ribozyme is a small RNA molecule that acts stoichiometrically to cleave multiple target RNA molecules [1]. This unique ability of a ribozyme to degrade multiple target RNA molecules is a more efficient approach for down regulating genes that are expressed at very high levels in cancer cells [2]. We had previously designed three anti-stathmin ribozymes that target the nucleotide triplets at positions 184 (GUC), 197 (GUU) and 305 (GUC) of the human stathmin mRNA [3]. We confirmed specificity of cleavage by these ribozymes *in vitro* in a cell-free system and demonstrated their ability to cleave a stathmin RNA substrate in a catalytic manner [3]. We developed recombinant adenoviral vectors to co-express the anti-stathmin ribozymes along with a GFP marker gene in prostate cancer cells [4]. We generated two adenoviral vectors to transfer the anti-stathmin ribozymes that cleave stathmin mRNA at the highest efficiency and a control adenovirus that does not have ribozyme sequences [4]. We tested these adenoviruses in LNCaP, one of the most widely used human prostate cancer cell lines. The efficiency of gene transfer into LNCaP cells was 90%, as determined by flow cytometric analysis of GFP fluorescence. Our studies showed that transduction of LNCaP cells with anti-stathmin ribozymes results in profound growth inhibition, G2-M

arrest, inhibition of anchorage independent colony formation and a marked increase in apoptosis [4]. Similar anti-mitotic and anti-proliferative effects were also observed in androgen-independent DU145 and PC3 human prostate cancer cell lines [4]. Thus, it is clear that the observed phenotypic effects of the anti-stathmin ribozymes on cell proliferation, mitotic arrest, and induction of apoptosis are not peculiarities of LNCaP cells and can be generalized to other human prostate cancer cells. The details of all of these experiments can be found in our published manuscript [4].

**2. Biological effects of combinations of chemotherapeutic agents with anti-stathmin ribozymes in human prostate cancer cells:** Conventional chemotherapy in advanced prostate cancer is not very effective because of inherent chemoresistance of the prostate cancer cell. Although taxol is active *in vitro* against prostate cancer cells, its effects *in vivo* in patients with prostate cancer have been very modest [5, 6]. We asked whether stathmin inhibition would chemosensitize prostate cancer cells to different chemotherapeutic agents. We used three different assays to investigate the interactions of four different chemotherapeutic drugs, including taxol, with the anti-stathmin ribozyme in prostate cancer cells. We studied the interaction of Ad.Rz305.GFP (moi of 5 pfu/cell) with microtubule interfering drugs like taxol (1-4 nM), topoisomerase inhibitors like etoposide [7] (0.25-2  $\mu$ M), and other chemotherapeutic agents that are less active in prostate cancer such as 5-FU (1-5  $\mu$ M) and adriamycin (2-10 nM). We investigated the effects of these agents on proliferation, clonogenicity and apoptosis in LNCaP cells in the presence and absence of stathmin inhibition. The concentrations of the different drugs that we used were determined empirically in pilot experiments and were significantly below the IC50.

In the first experiment, we evaluated the effects of different concentrations of chemotherapeutic drugs on the rate of proliferation of LNCaP cells in the presence and absence of anti-stathmin ribozyme (Fig.1). Exposure of uninfected LNCaP cells or cells infected with control Ad.GFP virus to taxol (4 nM), etoposide (2  $\mu$ M), 5-FU (5  $\mu$ M) or Adriamycin (10 nM) resulted in a modest decrease in proliferation. In contrast, exposure of cells infected with Ad.Rz305.GFP adenovirus to the same concentration of drugs resulted in a more profound decrease in proliferation. Impressively, exposure of Ad.Rz305.GFP infected cells to taxol or etoposide resulted in a complete loss of proliferation while exposure of the same infected cells to 5-FU or Adriamycin resulted in growth inhibition but the cells continued to proliferate. The same combinations were tested at different concentrations of chemotherapeutic agents. The observed growth inhibition of Ad.Rz305.GFP infected cells was always more profound in the presence of taxol and etoposide than in the presence of Adriamycin and 5-FU (data not shown). Thus, stathmin-inhibition results in greater sensitization of prostate cancer cells to the growth inhibitory effects of taxol and etoposide than to those of 5-FU or Adriamycin [8].

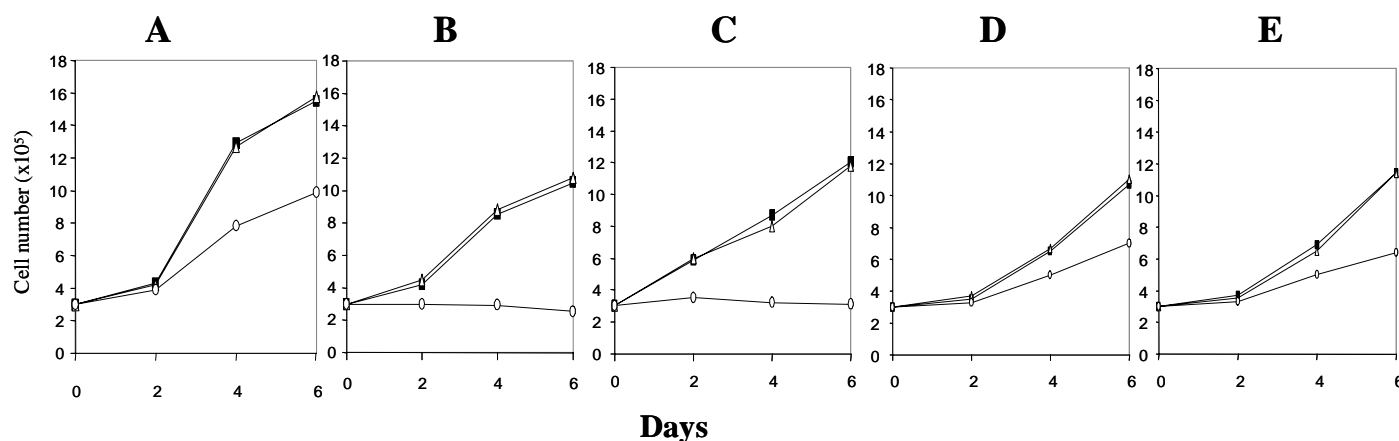


**Figure 1. Effects of combinations of chemotherapeutic agents with anti-stathmin therapy on proliferation of LNCaP.** Equal number of uninfected cells or cells infected with control Ad.GFP or anti-

stathmin Ad.Rz305.GFP viruses were exposed to different drugs at the specified concentrations. Viable cell counts were determined on alternate days in a hemocytometer. Uninfected cells are represented as open triangles and cells infected with either control Ad.GFP or Ad.Rz305.GFP adenoviruses are represented as closed rectangles and open circles respectively. (A) Growth curves of uninfected cells or cells infected with control Ad.GFP or Ad.Rz305.GFP in the absence of drug exposure. (B) Growth curves of uninfected cells or cells infected with control Ad.GFP or Ad.Rz305.GFP in the presence of taxol (4 nM). (C) Growth curves of uninfected cells or cells infected with the control Ad.GFP or the Ad.Rz305.GFP adenovirus in the presence of etoposide (2  $\mu$ M). (D) Growth curves of uninfected cells or cells infected with the control Ad.GFP or the Ad.Rz305.GFP adenovirus in the presence of 5-FU (5  $\mu$ M). (E) Growth curves of uninfected cells or cells infected with the control Ad.GFP or the Ad.Rz305.GFP adenovirus in the presence of Adriamycin (10 nM).

In the second experiment, we analyzed the effects of the combination of the anti-stathmin ribozyme with different chemotherapeutic agents on apoptosis using a TUNEL assay [8]. TUNEL analyses of uninfected or control Ad.GFP infected cells at a moi of 5 showed a modest degree of apoptosis, both in the absence (0.4%) and presence (2.5-3.1%) of different drugs. Interestingly, cells infected with Ad.Rz305.GFP at a moi of 5 showed 3.5% TUNEL positive cells in the absence of drug exposure. This increased to 6.6%, 6.9%, 22.2% and 25.6% when the infected cells were exposed to Adriamycin, 5-FU, etoposide and taxol, respectively [8]. In the third and final experiment, we examined the effects of the combination of anti-stathmin ribozyme with different chemotherapeutic agents on clonogenic growth in semi-solid medium. Clonogenicity of the uninfected LNCaP cells and of cells infected with the control Ad.GFP at a moi of 5 were moderately reduced (15-20%) after exposure to the different drugs [8]. In contrast, when Ad.Rz305.GFP infected cells (at the same moi) were exposed to taxol (4 nM) or etoposide (2  $\mu$ M), their clonogenicity was reduced by 98-99% [8]. Clonogenicity of the same Ad.Rz305.GFP-infected cells was reduced by 57% and 54%, respectively, upon exposure to 5-FU (5  $\mu$ M) or Adriamycin (10 nM) [8]. Thus, in all three assays, the combinations of the anti-stathmin ribozyme with taxol and etoposide were much more potent than its combinations with 5-FU and Adriamycin.

Since inhibition of clonogenic growth *in vitro* best predicts anti-tumor effects *in vivo* in nude mice, we used the median effect analyses method of Chou and Talalay [9] to determine if the effects of the combinations on clonogenicity are additive or synergistic (Fig.2). This method identifies an interaction as synergistic, additive or antagonistic by determining the difference between the observed combination effect and the expected additive effect. According to this method, a combination index (CI) of less than one denotes a synergistic interaction, a CI of around one denotes an additive interaction and a CI >1 indicates an antagonistic interaction [9]. We used the Calcsyn<sup>®</sup> software that uses the equations of the Chou and Talalay to assess the therapeutic interactions between the anti-stathmin adenovirus and different chemotherapeutic agents. This software takes into account both the potency (Dm values) and the shapes of the dose-effect curves (m values) to precisely analyze the combination effect of two agents. The CI values were determined to be <1 when the anti-stathmin adenovirus was combined with different concentrations of either taxol (1-6 nM) (Fig.2A) or etoposide (0.25-2  $\mu$ M) (Fig.2B). In contrast, the CI values were around 1 when the anti-stathmin adenovirus was combined with different concentrations of either adriamycin (1-10 nM) (Fig.2C) or 5-FU (0.5-5  $\mu$ M) (Fig.2D). Thus, this data is indicative of a synergistic interaction when the anti-stathmin adenovirus is combined with either taxol or etoposide and an additive interaction when the anti-stathmin adenovirus is combined with either adriamycin or 5-FU.

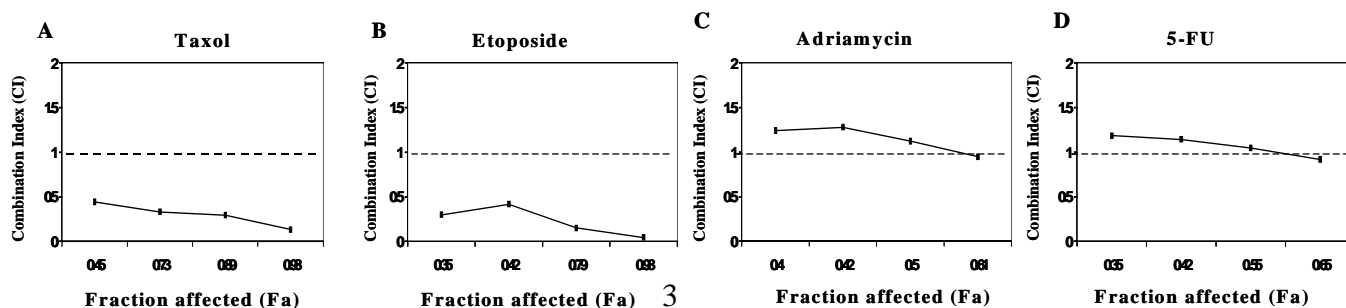


**Fig.2. Evaluation of combination effect of anti-stathmin adenovirus and different chemotherapeutic agents.** The Chou and Talalay combination index method was used to evaluate the therapeutic interactions between anti-stathmin adenovirus and different chemotherapeutic agents. The Fa-CI plots were constructed using the Calcsyn<sup>®</sup> software. (A) The Fa-CI plot represents the combination Index (CI) values and the fraction affected (Fa) at different concentrations of taxol (1-6 nM) in cells infected with the anti-stathmin adenovirus. (B) The Fa-CI plot represents the CI values and the Fa at different concentrations of etoposide (0.25-2  $\mu$ M) in cells infected with the anti-stathmin adenovirus. (C) The Fa-CI plot represents the CI values and the Fa at different concentrations of Adriamycin (1-10 nM) in cells infected with the anti-stathmin adenovirus. (D) The Fa-CI plot represents the CI values and the Fa at different concentrations of 5-FU (0.5-5  $\mu$ M) in cells infected with the anti-stathmin adenovirus. The additive effect of the combination of anti-stathmin adenovirus and the different drugs is represented at CI=1 (dashed line). A CI < 1 denotes synergistic interaction, a CI of around 1 denotes an additive interaction and a CI >1 indicates an antagonistic interaction.

We extended those studies by investigating the effects of a triple combination of anti-stathmin ribozyme with taxol and etoposide on proliferation, clonogenicity and apoptosis in LNCaP cells [8]. In these studies, we used low “sub-therapeutic” concentrations of taxol (1 nM) with etoposide (0.5  $\mu$ M), both of which have essentially no growth inhibitory effects in uninfected LNCaP cells or LNCaP cells infected with the control Ad.GFP virus (data not shown). Interestingly, exposure of Ad.Rz305.GFP infected cells to these same low concentrations of taxol and etoposide resulted in a complete loss of proliferation (data not shown). Similarly, Ad.Rz305.GFP infected cells exposed to low concentrations of taxol with etoposide showed virtually complete loss of clonogenicity (1-2% of baseline) while the clonogenicity of uninfected cells or cells infected with control Ad.GFP virus were modestly reduced to 80% of baseline following exposure to the same concentrations of taxol with etoposide (Fig. 3).

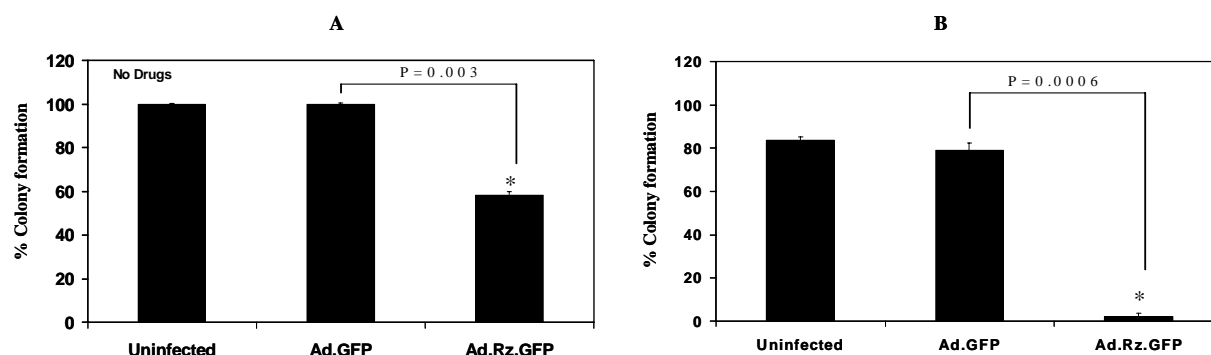


**Fig.3. Effects of triple combination of anti-stathmin adenovirus, taxol and etoposide on the clonogenic potential of LNCaP cells.** (A) Bar graph illustrates the clonogenicity of uninfected, control Ad.GFP and Ad.Rz.GFP infected cells at baseline in the absence of taxol and etoposide as indicated. (B) Bar graph illustrates the clonogenicity of uninfected, control Ad.GFP and Ad.Rz.GFP infected cells in the presence of non-inhibitory concentrations of taxol (1 nM) and etoposide (0.5  $\mu$ M) as indicated. Error bars represent the standard deviation calculated from three different experiments. Statistical significance was determined using Student's t test.

Similarly, in an apoptosis assay, exposure of uninfected cells and cells infected with control Ad.GFP virus to taxol with etoposide resulted in only 2-3% TUNEL positive cells. In contrast, Ad.Rz305.GFP infected cells showed a marked increase in the fraction of TUNEL positive cells (38%) upon exposure to taxol with etoposide [8]. Thus, anti-stathmin ribozyme can markedly enhance the effects of low non-

inhibitory concentrations of taxol and etoposide to result in profound inhibition of proliferation, clonogenicity and apoptosis. Since taxol and etoposide are the two most active chemotherapeutic agents in prostate cancer, this triple low-dose combination may provide a highly effective form of combination therapy that would avoid toxicities associated with the use of multiple chemotherapeutics at maximally tolerated doses. The details of all of these experiments can be found in our published manuscript [8].

**3. Biological effects of anti-stathmin ribozymes on prostate cancer xenografts in nude mice:** We performed two sets of experiments to examine the effects of anti-stathmin ribozyme on tumor growth *in vivo* [10]. In the first experiment, we divided six nude mice into three groups, each consisting of two mice. Group I was injected subcutaneously at four different sites as described [11] with  $1 \times 10^7$  uninfected LNCaP cells. Group II was injected subcutaneously at four different sites with  $1 \times 10^7$  LNCaP cells pre-infected with control Ad.GFP adenovirus at moi of 25. Similarly, group III was injected subcutaneously at four different sites with  $1 \times 10^7$  cells pre-infected with anti-stathmin Ad.Rz305.GFP adenovirus at moi of 25. The Ad.GFP or Ad.Rz305.GFP infected cells that were injected in the two groups of mice had transduction efficiencies in the range of 80-90%, as determined by GFP fluorescence analyses (data not shown). We monitored the mice closely for development of tumors, and when tumors formed, we measured tumor size every five days for two months. The two groups of mice that were injected with both uninfected cells (group I) and with cells infected with control Ad.GFP (group II) formed tumors at all injection sites. These tumors ranged in diameter from 0.3 to 1.4 cm. In contrast, the group of mice that were injected with cells infected with the anti-stathmin adenovirus (group III) failed to form tumors at any of the injection sites by the time the experiment was terminated after 60 days.

In a second set of experiments, we examined the therapeutic efficacy of the anti-stathmin adenovirus in established tumors derived from uninfected LNCaP cells. Eight animals were injected subcutaneously at four sites each with  $5 \times 10^6$  LNCaP cells/site. We initiated treatment by intratumoral injections after the mice developed tumors that measured from 0.4-0.7 cm in diameter. In each mouse, the two tumors on the left flank were injected intratumorally with either PBS or with the control Ad.GFP virus ( $10^{10}$  viral particles, once every 5 days, for a total of 3 injections) while the two tumors on the right flank were injected with the anti-stathmin adenovirus ( $10^{10}$  viral particles, once every 5 days, for a total of 3 injections). Intratumoral injections were given at multiple locations within each tumor. The animals were closely monitored for the rate of tumor growth. Tumor sizes were measured every 5 days and relative tumor volumes were estimated by multiplying the longest diameter by the square of the shortest diameter and dividing by two [11]. Figure 4 shows representative data from 4 tumors that were injected either with PBS (Fig. 4A), control adenovirus (Fig. 8B), or Ad.Rz305.GFP (Fig. 4C & 4D). As illustrated, tumors injected with PBS or the control adenovirus continued to grow, while those injected with Ad.Rz305.GFP either stopped growing completely (Fig. 4C) or totally regressed (Fig. 4D). Figure 5 summarizes the findings of the *in vivo* studies of tumorigenicity in the nude mice that were used in this experiment. The relative tumor volumes were plotted at the initiation of the experiment (i.e. at the time of adenoviral injections) and at the termination of the experiment 60 days later. Seventy percent of the tumors injected with the ribozyme carrying adenovirus regressed completely and 30% stopped increasing in size after the injections. In contrast, tumors that were injected with PBS or the control adenovirus continued to grow and reached large sizes. The mice were sacrificed if the tumors invaded the skin and caused ulceration before the experiment was terminated at 60

days.

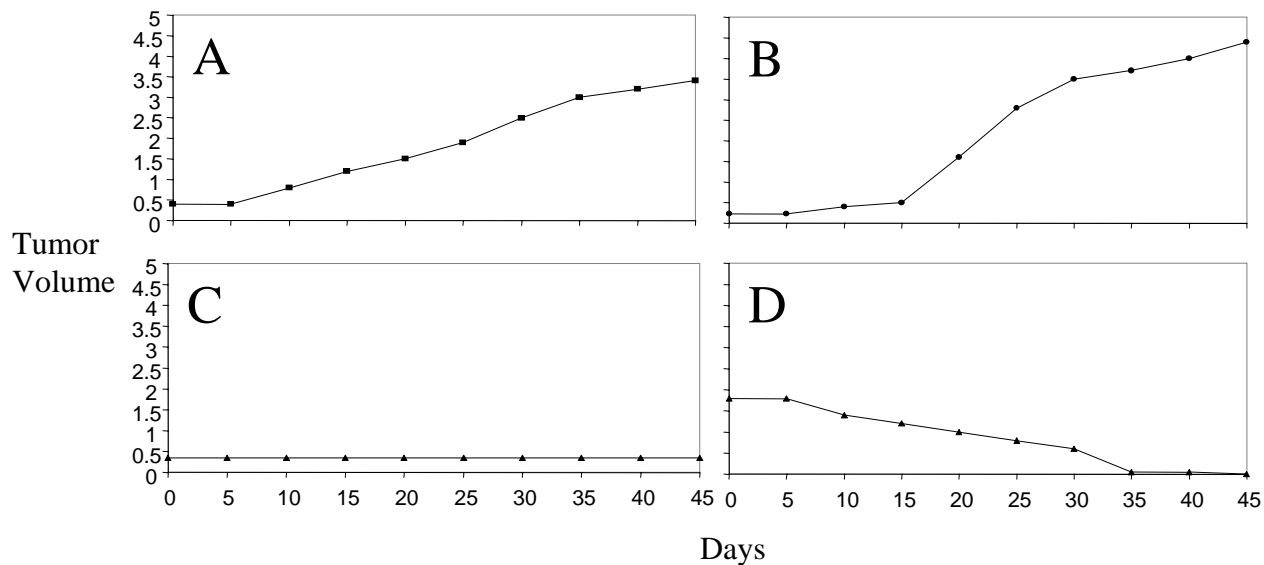


**Figure 4. Effects of anti-stathmin ribozyme in LNCaP xenografts in nude mice.** Mice with established tumors were injected with either PBS, control Ad.GFP or Ad.Rz305.GFP and tumor volumes were determined every 5 days. (A) A representative graph that shows a progressive increase in the rate of tumor growth after injection with PBS. (B) A representative graph that shows progressive increase in the rate of tumor growth after injection with the control Ad.GFP adenovirus. (C) A representative graph that shows complete inhibition of tumor growth after injection with the Ad.Rz305.GFP adenovirus. (D) A representative graph that shows tumor regression after injection with the Ad.Rz305.GFP adenovirus.

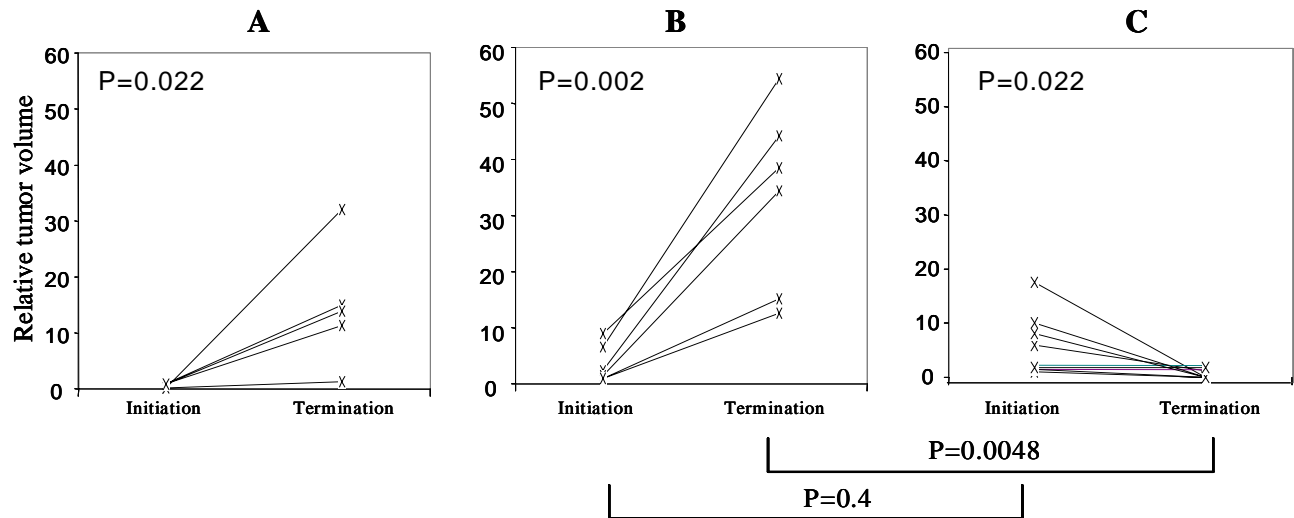


**Figure 5. Effects of anti-stathmin ribozymes in LNCaP xenografts in nude mice.** Mice with established tumors were injected with either PBS, control Ad.GFP or Ad.Rz305.GFP. Initiation refers to the day the first injection was administered and Termination refers to the day the experiment ended. (A) This graph represents changes in the relative tumor volumes after injection with PBS. (B) This graph represents changes in relative tumor volumes after injections with the control Ad.GFP adenovirus. (C) This graph represents changes in relative tumor volumes after injection with the Ad.Rz305.GFP adenovirus. The *P* values were calculated using the student's T test.

We performed statistical analysis to determine the significance of the observed differences in the size of the tumors that were injected with the different agents. The p-value for the increase in the size of tumors injected with PBS between Initiation and Termination is 0.022. Similarly, the p-value for the increase in the size of tumors injected with the control Ad.GFP between Initiation and Termination is 0.022. More importantly, p-value for the decrease in the size of tumors injected with Ad.Rz305.GFP adenovirus between Initiation and Termination is 0.022. We also performed analysis of the differences in tumor sizes between groups. The size of the tumors that were injected with Ad.GFP and Ad.Rz305.GFP were not significantly different at the Initiation of the experiment ( $p=0.4$ ). In contrast, the differences in the sizes of the tumors at the termination of the experiments were highly significant ( $p=0.0048$ ). Therefore, the differences between the observed increases in the size of tumors injected with the control virus or PBS as opposed to the decrease in the sizes of tumors injected with the anti-stathmin adenoviruses are all statistically significant.

## C. KEY RESEARCH ACCOMPLISHMENTS

The experiments described above demonstrate that the anti-stathmin adenoviruses can markedly inhibit the proliferation and clonogenicity of prostate cancer cells and can induce significant apoptosis. They also demonstrate that combination of the anti-stathmin adenovirus with chemotherapeutic agents like taxol or etoposide can result in a synergistic anti-tumor effect while combination of the anti-stathmin adenovirus with 5-FU or adriamycin can result in an additive anti-tumor effect. Our studies also demonstrate that the anti-stathmin adenovirus can inhibit tumor growth in mouse models of human prostate cancer.

## D. REPORTABLE OUTCOMES

The research summarized in this annual progress report was presented every year at the National Meeting of the American Association of Cancer Research during the period of funding. The abstracts that were presented are as follows:

1. Misry, SJ, Bank A, Atweh, GF. *Cell cycle inhibition therapy: Stathmin as a potential therapeutic target in prostate cancer. Proceedings of the American Association of Cancer Research, Abstract #3039, 2004.*
2. Mistry, SJ, Perez Y, Atweh, GF. *Therapeutic interactions of anti-stathmin therapy with chemotherapeutic agents in prostate cancer. Proceedings of the American Association of Cancer Research, Abstract #4940, 2005.*
3. Mistry, SJ, Atweh, GF. *Microtubule targeting therapy: Anti-stathmin based molecular cancer therapeutic in vivo. Proceedings of the American Association of Cancer Research, Abstract # 524, 2006.*

Two manuscripts describing this work have recently been published and one manuscript describing the in vivo studies is currently in preparation.

1. Mistry SJ, Bank A, Atweh GF. *Targeting stathmin in prostate cancer. Molecular Cancer Therapeutics* 2005; 4:1821-1829.
2. Mistry SJ, Atweh, GF. *Therapeutic interaction between stathmin inhibition and chemotherapeutic agents in prostate cancer.* 2006; 5(12): 3248-3257.
3. Mistry SJ, Atweh, GF. *Anti-stathmin therapy in mouse models of human prostate cancer, 2007 (manuscript in preparation).*

## E. CONCLUSIONS

Our studies have demonstrated that the anti-stathmin adenoviruses can mediate anti-proliferative and anti-tumorigenic effects *in vitro* and *in vivo* models of human prostate cancer. We have also shown that the combination of stathmin inhibition with chemotherapeutic agents can result in synergistic anti-tumor activity against prostate cancer cells. Thus, these studies provide the proof-of-principle that stathmin is as an attractive target for prostate cancer therapy.

## F. REFERENCES

1. Kijima, H., Ishida, H., Ohkawa, T., Kashani-Sabet, M., Scanlon, K. J., *Therapeutic applications of ribozymes*. Pharmacol Ther, 1995. **68**(2): p. 247-67.
2. Irie A, B.D., Scanlon KJ, *Ribozyme-mediated cancer gene therapy*. Int. J Urol., 1997. **4**: p. 329-337.
3. Mistry, S., Benham, CJ., Atweh, GF., *Development of ribozymes that target stathmin, a major regulator of the mitotic spindle*. Antisense Nucleic Acid Drug Dev, 2001. **11**: p. 41-9.
4. Mistry, S.J., Bank, A., Atweh, G.F., *Targeting stathmin in prostate cancer*. Molecular Cancer Therapeutics, 2005. **4**: p. 1821-1829.
5. Roth, B., Yeap, BY., Wilding, G., Kasimis, B., McLeod, D., Loehrer, PJ., *Taxol in advanced, hormone-refractory carcinoma of the prostate. A phase II trial of the Eastern Cooperative Oncology Group*. Cancer, 1993. **72**: p. 2457-60.
6. Kang, M., Figg, WD., Dahut, W., *Taxanes in hormone-refractory prostate cancer*. Cancer Pract, 1999. **7**: p. 270-2.
7. Salido, M., L.J., Lopez, A., Vilces, J., Aparicio, J., *Etoposide sensitivity of human prostate cancer cell lines PC-3, DU145 and LNCaP*. Histol Histopathol., 1999. **14**: p. 125-134.
8. Mistry, S.J., Atweh, G.F., *Therapeutic interactions between stathmin inhibition and chemotherapeutic agents in prostate cancer*. Mol Cancer Ther, 2006. **5**: p. 3248-3257.
9. Chou, T.C., and Talalay, P., *Quantitative analysis of dose effect relationships: the combined effects of multiple drugs or enzyme inhibitors*. Adv. Enzyme Regul., 1984. **22**: p. 27-55.
10. Mistry SJ, A.G., *Microtubule targeting therapy: Anti-stathmin based molecular cancer therapeutics in vivo*. Proceedings of the American Association of Cancer Research, 2006. Abstract # 524.
11. Luo, X.N., et al., *The tumor suppressor gene WT1 inhibits ras-mediated transformation*. Oncogene, 1995. **11**(4): p. 743-50.

# Targeting stathmin in prostate cancer

Sucharita J. Mistry, Alexander Bank,  
and George F. Atweh

Division of Hematology-Oncology, Department of Medicine,  
Mount Sinai School of Medicine, New York, New York

## Abstract

**Stathmin is the founding member of a family of microtubule-destabilizing proteins that regulate the dynamics of microtubule polymerization and depolymerization. Stathmin is expressed at high levels in a variety of human cancers and provides an attractive molecule to target in cancer therapies that disrupt the mitotic apparatus. We developed replication-deficient bicistronic adenoviral vectors that coexpress green fluorescent protein and ribozymes that target stathmin mRNA. The therapeutic potential of these recombinant adenoviruses was tested in an experimental androgen-independent LNCaP prostate cancer model. Adenovirus-mediated transfer of anti-stathmin ribozymes resulted in efficient transduction and marked inhibition of stathmin expression in these cells. Cells that were transduced with the anti-stathmin adenoviruses showed a dramatic dose-dependent growth inhibition. This was associated with accumulation of LNCaP cells in the G<sub>2</sub>-M phases of the cell cycle. A similar dose-dependent inhibition of clonogenic potential was also observed in cells infected with anti-stathmin adenoviruses. Morphologic and biochemical analysis of infected cells showed a marked increase in apoptosis characterized by detachment of the cells, increased chromatin condensation, activation of caspase-3, and fragmentation of internucleosomal DNA. If these findings are confirmed *in vivo*, it may provide an effective approach for the treatment of prostate cancer. [Mol Cancer Ther 2005; 4(12):1821–9]**

## Introduction

Microtubules are dynamic protein polymers that are essential for a myriad of cellular functions, including

mitosis, intracellular transport, polarity, and motility (1). During cell division, the mitotic spindle, which is composed of microtubule polymers of  $\alpha/\beta$ -tubulin heterodimers, plays the primary role in the segregation of chromosomes to the two daughter cells (1). The movement of chromosomes toward the spindle poles is made possible by the dynamic instability of microtubules that switch between phases of elongation and shortening (1, 2). The transition from a phase of growth to a phase of shrinkage is called catastrophe, and the transition from a phase of shrinkage to a phase of growth is called rescue (1). The dynamics of microtubule polymerization/depolymerization during the different phases of the cell cycle are regulated by a balance between the activities of two major classes of proteins, microtubule-stabilizing and microtubule-destabilizing factors (2). Changes in the phosphorylation of these proteins are responsible for cell cycle-specific alterations of the microtubule network.

Stathmin is a founding member of a family of microtubule-destabilizing proteins that play a critical role in the regulation of mitosis (3–5). The initial clue that stathmin may have a direct role in the regulation of mitosis came from genetic studies that showed that manipulation of stathmin expression interferes with the progression of cells through mitosis (6, 7). High levels of stathmin expression were described in a variety of human malignancies, including acute leukemia (8), malignant lymphoma (9), neuroblastoma (10), ovarian carcinoma (11), prostate carcinoma (12), and breast carcinoma (13, 14). Interestingly, in many of these cancers, a high level of stathmin expression was shown to correlate with bad prognosis (12, 13, 15). This suggested that a high level of stathmin expression may play an important role in the malignant phenotype. We have shown previously that plasmid-mediated antisense inhibition of stathmin expression in K562 leukemic cells results in abrogation of the malignant phenotype (16). These observations led us to propose that stathmin may be an attractive new target for cancer therapeutics whose aim is to disrupt microtubule dynamics and the mitotic spindle.

Although stathmin is expressed at high levels in a variety of human cancers, we believe that prostate cancer provides one of the best models for the development of therapeutics that target stathmin. When biopsy specimens from human prostate cancers were immunostained with an anti-stathmin antibody, immunoreactivity was seen in poorly differentiated tumors but not in hyperplastic or highly differentiated prostate cancer (12). More importantly, the level of expression of stathmin was shown to correlate with the malignant behavior of prostate cancer cells (12). In fact, it was proposed that the level of expression of stathmin may serve as an important prognostic marker in prostate cancer (12). The fact that the prostate is relatively accessible for local injections adds to the attractiveness of this model for the local delivery of a therapeutic gene that targets stathmin expression.

Received 6/29/05; revised 9/8/05; accepted 10/13/05.

**Grant support:** Derald Ruttenberg Cancer Center Career Development Award (S.J. Mistry) and Department of Defense Prostate Cancer Research Program grant W81XWH-04-1-0219 (G.F. Atweh).

The costs of publication of this article were defrayed in part by the payment of page charges. This article must therefore be hereby marked advertisement in accordance with 18 U.S.C. Section 1734 solely to indicate this fact.

**Requests for reprints:** Sucharita J. Mistry or George F. Atweh, Division of Hematology-Oncology, Department of Medicine, Mount Sinai School of Medicine, One Gustave L. Levy Place, New York, NY 10029. Phone: 212-241-5293; E-mail: sucharita.mistry@mssm.edu or george.atweh@mssm.edu

Copyright © 2005 American Association for Cancer Research.

doi:10.1158/1535-7163.MCT-05-0215

In a previous study, we designed and tested several ribozymes that target and degrade stathmin mRNA (17). A major advantage of ribozymes over other RNA-interfering strategies is that ribozymes cleave target mRNA catalytically, resulting in highly efficient mRNA degradation, thus providing a more efficient approach for down-regulating genes like stathmin that are expressed at high levels in cancer cells (18, 19). We tested three different hammer-head ribozymes that targeted two GUC motifs at nucleotides 184 (Rz184) and 305 (Rz305) and a GUU motif at nucleotide 197 (Rz197) of stathmin mRNA (17). Rz184 and Rz305 showed efficient catalytic cleavage of stathmin mRNA *in vitro*, whereas Rz197 was significantly less efficient (17). In this report, we describe the generation and characterization of adenoviral vectors that carry genes encoding Rz184 and Rz305. Our studies show that these recombinant adenoviruses can degrade stathmin mRNA efficiently in prostate cancer cells and result in marked inhibition of their proliferation and clonogenicity and increase in apoptosis.

## Materials and Methods

### Cell Lines

The human androgen-independent LNCaP prostate cancer cells used in this study were described previously (20). These cells were grown in RPMI 1640 supplemented with 10% charcoal-stripped fetal bovine serum, 5 µg/mL human insulin, 100 units/mL penicillin, and 100 µg/mL streptomycin. The 293 packaging cell line was maintained in DMEM supplemented with 10% fetal bovine serum, 100 units/mL penicillin, and 100 µg/mL streptomycin. The cells were maintained at 37°C in a humidified 5% CO<sub>2</sub> environment.

### Production of Recombinant Adenoviruses

The first step in the generation of the recombinant adenoviruses involved cloning of the anti-stathmin ribozyme genes, Rz184 and Rz305 (17), in adenoviral transfer vectors. The oligonucleotides encoding Rz184 and Rz305 (17) were flanked by *Bgl*II restriction sites to facilitate cloning at the unique *Bgl*II site of the adenoviral transfer vector, pAd-CMV5-IRES-GFP (Quantum Technology, Montreal, Canada). All recombinant transfer plasmids were verified for the correct insertion of anti-stathmin ribozyme sequences by DNA sequencing. To generate a control virus, we used a similar adenoviral backbone in which the GFP coding sequences were placed under the control of the CMV5 promoter without the ribozyme sequences.

The second step involved the production of infectious viral particles by standard homologous recombination (21). This was achieved by cotransfection of each of the recombinant transfer plasmids with part of the adenovirus type 5 genome selected to promote *in vivo* homologous recombination between the two DNA molecules to yield infectious virus. Cotransfection of the recombinant transfer plasmid and the E1a-deleted adenoviral DNA was facilitated by calcium phosphate coprecipitation on 293 packaging cells, which complement the E1a and E1b adenovirus

type 5 viral genes that are deleted from the recombinant adenoviruses. Recombinant adenoviruses were identified by screening of packaging cells for bright green plaques under a fluorescent microscope. Several individual plaques were picked for each virus and their viral lysates were analyzed by PCR for the presence of anti-stathmin ribozyme sequences in the adenovirus type 5 genome. Several adenoviral clones were positive for both anti-stathmin ribozyme and GFP sequences. For large-scale production of the virus, a single clone from each recombinant adenovirus was amplified in 293 cells and purified by ultracentrifugation on a cesium chloride gradient, dialyzed, and stored at -80°C. The infectious viral titers were determined by plaque assays in 293 cells (21).

### Adenoviral Infections *In vitro*

Cells were seeded in six-well culture plates 24 hours before virus infection. For all the experiments described below, cells were infected with the recombinant adenoviruses at different multiplicity of infection (MOI) in a 2% reduced serum medium for 3 hours. After infection, the virus was removed and the cells were further incubated in complete growth medium. The efficiency of the adenoviral infections was assessed by fluorescence microscopy or flow cytometry at either 48 or 72 hours after infection.

### Northern Analysis

Uninfected cells and cells infected with either control Ad.GFP, Ad.Rz184.GFP, or Ad.Rz305.GFP adenoviruses at MOI of 25 were harvested at 24, 48, or 72 hours. Total RNA was isolated from these cells using the guanidinium thiocyanate-phenol-chloroform extraction method (22). Each RNA sample (20 µg) was denatured in glyoxal and separated by agarose gel electrophoresis as described (22). A 1.5-kb *Xba*I fragment from the stathmin cDNA (23) was labeled by random priming and used as a probe in hybridization experiments. The Northern filter was stripped and rehybridized to ribozyme, GFP, and 18S rRNA probes.

### Western Analysis

Uninfected cells and cells infected with either control Ad.GFP, Ad.Rz184.GFP, or Ad.Rz305.GFP adenoviruses at MOI of 25 were harvested 72 hours after infection. The cell pellets were lysed for 30 minutes on ice in a buffer consisting of 50 mmol/L Tris (pH 7.4), 150 mmol/L NaCl, and 1% Triton X-100. The cell extracts were clarified by centrifugation and the protein concentrations were determined by using the Bio-Rad protein assay kit (Bio-Rad, Hercules, CA). Each protein extract (25 µg) was electrophoresed on a 15% SDS-polyacrylamide gel, transferred to membrane, and blocked in PBS containing 5% nonfat milk powder and 0.2% Tween 20 for 1 hour at room temperature. The filter was incubated overnight at 4°C with anti-stathmin antibody (BD PharMingen, San Diego, CA) in PBS containing 0.1% Tween 20 followed by incubation with horseradish peroxidase-conjugated anti-mouse IgG (Sigma, St. Louis, MO) for 1.5 hours. The filter was then washed several times with PBS containing 0.2% Tween 20. As an internal control, the same filter was hybridized to anti-actin antibody (Oncogene Research Products,

San Diego, CA) followed by incubation with horseradish peroxidase-conjugated anti-mouse IgM (Calbiochem, San Diego, CA) as above. The bands were visualized by chemiluminescence using an enhanced chemiluminescence kit (Amersham Biosciences, Piscataway, NJ).

#### Cell Proliferation Assay

To assess the rate of proliferation, equal numbers of cells ( $2 \times 10^5$ ) were infected with either control or anti-stathmin adenoviruses in triplicates at different MOIs. The cells (floating and detached) were harvested and stained with trypan blue to determine cell viability. Cells were counted on a hemocytometer on alternate days and the data were plotted in graphical form to generate growth curves.

#### Cell Cycle Analysis

We used propidium iodide staining of fixed whole cells to analyze the distribution of cells in the different phases of the cell cycle (4). Uninfected cells and cells infected with either control or anti-stathmin adenoviruses at different MOIs were harvested and divided into two fractions, one for cell cycle analysis and the other for GFP fluorescence analysis. For cell cycle analysis, the cells were fixed in 70% ethanol, washed in PBS, and resuspended in 1 mL propidium iodide solution (PBS containing 0.05 mg/mL, 0.1% sodium citrate and 1  $\mu$ g/mL RNase). The cells were incubated for 30 minutes at 37°C. DNA content was analyzed within 2 hours in a Becton Dickinson (Bedford, MA) FACStar Plus flow cytometer at 488 nm single laser excitation. For GFP fluorescence analysis, the cells were fixed in 1% paraformaldehyde. Transduction efficiencies of infected cells were assessed by measuring the fraction of cells that expressed GFP by flow cytometry. The cell cycle distribution and GFP positivity were analyzed using Win List software.

#### Clonogenic Assay

Anchorage-independent growth was assessed by colony formation in a methylcellulose semisolid medium. Equal numbers of cells were infected with either control or anti-stathmin adenoviruses in triplicates at MOI of 5, 10, and 25 for 3 hours. The cells were washed in PBS and resuspended in 5 mL methylcellulose-based semisolid medium (0.9% methylcellulose, 1% bovine serum albumin, and 0.1 mmol/L  $\beta$ -mercaptoethanol prepared in RPMI 1640 containing 30% fetal bovine serum, 100 units/mL penicillin, and 100  $\mu$ g/mL streptomycin). Cells ( $1 \times 10^4$ ) were then plated in six-well tissue culture plates in triplicates and incubated at 37°C in 5% CO<sub>2</sub> atmosphere. The colonies that formed were counted after 2 weeks.

#### Apoptosis Assays

Cells were infected with either control or anti-stathmin adenoviruses as above. Both floating and attached cells were harvested 5 days after infection and the effect of ribozyme-mediated stathmin inhibition on apoptosis was quantified in several different assays.

**Analysis of Nuclear Morphology.** For the morphologic evaluation of the proportion of apoptotic cells, ~10,000 uninfected and infected cells were spun onto a microscope slide and stained with 4',6-diamidino-2-phenylindole at

1  $\mu$ g/mL for 15 minutes. The cells were then scored under a fluorescence microscope as either normal (nuclei with smooth and homogeneous staining) or apoptotic (condensed nuclei with intense chromatin staining).

**Analysis of Caspase-3 Activation.** To detect caspase-3 activation, uninfected cells and cells infected with either Ad.GFP, Ad.Rz184.GFP, or Ad.Rz305.GFP were harvested, fixed, and permeabilized using a caspase-3 apoptosis kit according to the manufacturer's protocol (BD PharMingen). Cells were then stained with a monoclonal anti-caspase-3 antibody conjugated to phycoerythrin and analyzed by flow cytometry.

**Analysis of DNA Fragmentation.** DNA fragmentation was assessed by terminal deoxynucleotidyl transferase-mediated dUTP nick end labeling (TUNEL) assay using a Cell Death Detection kit (Roche) according to the manufacturer's instructions. Briefly, uninfected cells and cells infected with either Ad.GFP, Ad.Rz184.GFP, or Ad.Rz305.GFP were fixed, permeabilized, and incubated with the TUNEL reaction mixture. As a positive control, uninfected cells were treated with DNase. The free 3'-OH groups of fragmented DNA labeled with tetramethylrhodamine-labeled nucleotides were quantified by flow cytometry.

## Results

### Generation of Recombinant Adenoviruses That Carry Anti-Stathmin Ribozymes

The production of the recombinant adenoviruses was done in two steps. The first step involved the cloning of the anti-stathmin ribozymes in the adenoviral transfer vector. We used a bicistronic expression vector (pAd-CMV5-IRES-GFP) that contains an adenovirus origin of replication and 2.5 kb of human adenovirus type 5 DNA for efficient homologous recombination. This vector also contains an internal ribosome entry site element derived from the encephalomyocarditis virus that permits the translation of two open reading frames from the same mRNA (24). The internal ribosome entry site expression cassette of this vector is downstream from a unique cloning site to allow coexpression of a GFP selectable marker and the therapeutic gene of interest. Both the selectable and the therapeutic genes are placed under the control of CMV5, a CMV promoter-enhancer modified for maximal expression. This arrangement allows high-level expression of the transgene and easy visualization and/or selection of transduced cells.

We cloned the genes that encode Rz184 and Rz305 in the adenoviral gene transfer vectors as shown in Fig. 1. We tested the activity of these recombinant adenoviruses in an *in vitro* model of prostate cancer. The human LNCaP is the most widely used cell line for the study of prostate cancer (25). For our studies, we used an androgen-independent human LNCaP cell line that was derived by maintaining androgen-dependent LNCaP cells in an androgen-poor medium (20). This selective pressure led to the growth of androgen-independent cells with properties that mimic advanced prostate cancer (20).

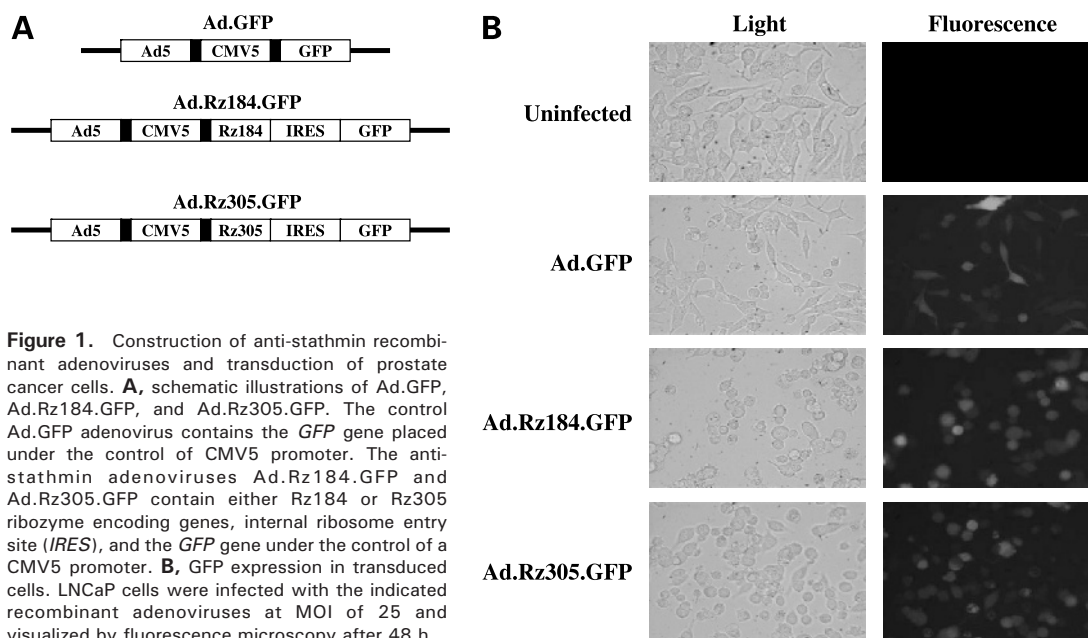


**Figure 1.** Construction of anti-stathmin recombinant adenoviruses and transduction of prostate cancer cells. **A**, schematic illustrations of Ad.GFP, Ad.Rz184.GFP, and Ad.Rz305.GFP. The control Ad.GFP adenovirus contains the *GFP* gene placed under the control of CMV5 promoter. The anti-stathmin adenoviruses Ad.Rz184.GFP and Ad.Rz305.GFP contain either Rz184 or Rz305 ribozyme encoding genes, internal ribosome entry site (*IRES*), and the *GFP* gene under the control of a CMV5 promoter. **B**, GFP expression in transduced cells. LNCaP cells were infected with the indicated recombinant adenoviruses at MOI of 25 and visualized by fluorescence microscopy after 48 h.

The efficiency of adenovirus infection was assessed by infecting the LNCaP cells with anti-stathmin adenoviruses at increasing MOI. As controls, the cells were either mock infected or infected with the control Ad.GFP adenovirus at a similar MOI to determine if adenoviral infection results in cytotoxicity. The efficiency of gene transfer was determined by quantifying the fraction of cells that expressed GFP by flow cytometry. Infection of cells with control or anti-stathmin adenoviruses at increasing MOIs from 5 to 50 resulted in a progressive increase in the percentage of transduced cells. The optimal MOI for LNCaP cells was determined to be between 5 and 25. Infection at these MOIs resulted in efficient transduction without any significant cytotoxicity. Figure 1B represents fluorescent microscopy images showing >90% of the cells in the monolayer culture positive for GFP fluorescence after a single infection with the recombinant adenoviruses at MOI of 25.

#### Effect of Anti-Stathmin Ribozymes on Stathmin Expression

We first asked whether adenovirus-mediated gene transfer of anti-stathmin ribozyme would decrease the level of stathmin mRNA in LNCaP cells. We did a time course analysis in which cells were harvested at different intervals after infection with either the control adenovirus or one of the two anti-stathmin adenoviruses (Fig. 2). Figure 2A and B shows Northern blots of RNA harvested at 24, 48, or 72 hours after infection. The level of stathmin mRNA was normalized to 18S rRNA to adjust for differences in RNA loading. The cells transduced with Ad.Rz305.GFP showed a modest decrease in the level of stathmin RNA after 24 hours (Fig. 2A, lane 3). The decrease in stathmin mRNA became more pronounced at 48 hours (69.2%; Fig. 2A, lane 5) and 72 hours (75.6%; Fig. 2A, lane 7). Similarly, the decrease in stathmin mRNA in cells

transduced with Ad.Rz184.GFP became more pronounced at 48 hours (58.8%; Fig. 2B, lane 5) and 72 hours (80.2%; Fig. 2B, lane 7). In contrast, cells transduced with the control Ad.GFP adenovirus did not show a significant decrease in the level of stathmin mRNA during the same period (Fig. 2A and B, lanes 2, 4, and 6). The progressive decrease in the level of stathmin mRNA correlated with the progressive increase in the level of anti-stathmin ribozymes (Fig. 2A and B). The same filter was also hybridized with a GFP probe as a surrogate for anti-stathmin ribozyme expression because both sequences are in the same polycistronic mRNA transcript (Fig. 2A and B). Western blot analysis showed a 74% and 86% reduction in the level of stathmin in Ad.Rz305.GFP-infected and Ad.Rz184.GFP-infected cells, respectively, relative to the uninfected or control Ad.GFP-infected cells. Thus, both Ad.Rz184.GFP and Ad.Rz305.GFP can efficiently down-regulate stathmin mRNA and protein levels in transduced LNCaP cells.

#### Effect of Anti-Stathmin Ribozymes on Proliferation

We examined the effects of the anti-stathmin ribozymes on the proliferation of LNCaP cells. Figure 3 illustrates the growth rates of uninfected cells, cells infected with the control Ad.GFP, and cells infected with either Ad.Rz184.GFP or Ad.Rz305.GFP adenoviruses. When cells were infected with Ad.GFP virus at different MOIs, no significant growth inhibition was observed compared with uninfected cells (Fig. 3A). In contrast, cells transduced with Ad.Rz184.GFP (Fig. 3B) or Ad.Rz305.GFP (Fig. 3C) showed a dose-dependent growth inhibition, with essentially complete cessation of growth at a MOI of 25.

We also observed striking differences in the morphology of cells transduced with anti-stathmin adenoviruses. A vast majority of the cells infected with anti-stathmin adenoviruses rounded up and detached from the culture dish after 3 to 4 days (data not shown). The rounding up and the

detachment of cells in culture are typical of mitotic cells that undergo profound cytoskeletal changes. In contrast, cells infected with the control adenovirus remained attached as a monolayer.

#### Effect of Anti-Stathmin Ribozymes on Cell Cycle Progression

We also examined the effects of adenovirus-mediated transduction of LNCaP cells with anti-stathmin ribozymes on cell cycle progression. Cells were infected with either control Ad.GFP, Ad.Rz184.GFP, or Ad.Rz305.GFP adenoviruses at different MOIs. After 48 hours, the cells were harvested and stained with propidium iodide and their DNA content was assessed in a flow cytometer (Fig. 4). When LNCaP cells were transduced with the control Ad.GFP at different MOIs, the DNA histograms were similar to that of uninfected cells (Fig. 4A). In contrast, cells transduced with Ad.Rz184.GFP or Ad.Rz305.GFP showed a marked accumulation of cells in the G<sub>2</sub>-M phases, with a corresponding decrease in the fraction of cells in the G<sub>0</sub>-G<sub>1</sub> phases of the cell cycle (Fig. 4A). Moreover, the accumulation of cells in the G<sub>2</sub>-M phases in the infected cells increased with increase in MOI.

To make sure that the observed differences in the DNA histograms are not a result of differences in the efficiency of viral transduction, we quantified the transduction efficiency directly by measuring the fraction of cells that express GFP. Small aliquots of cells from the experiment described above were fixed in 1% paraformaldehyde and analyzed for GFP fluorescence by flow cytometry. The fractions of GFP-positive (i.e., transduced) cells were comparable in cells infected with Ad.GFP, Ad.Rz184.GFP, and Ad.Rz305.GFP (Fig. 4B). Thus, the observed differences in the cell cycle distribution of transduced cells are clearly not a result of differences in the efficiency of transduction.

#### Effect of Anti-Stathmin Ribozymes on Clonogenicity

We also studied the effects of anti-stathmin adenoviruses on the ability of LNCaP cells to form anchorage-independent colonies in semisolid medium. Figure 5 illustrates the relative clonogenicity of uninfected cells and cells infected with either Ad.GFP, Ad.Rz184.GFP, or

Ad.Rz305.GFP adenoviruses at different MOIs. No significant differences in the clonogenicity were seen when uninfected cells were compared with cells infected with the control Ad.GFP adenovirus (Fig. 5). In contrast, LNCaP cells infected with anti-stathmin adenoviruses at different MOIs showed a dose-dependent inhibition of colony formation, with a near-complete suppression of anchorage-independent growth at a MOI of 25. Thus, adenovirus-mediated anti-stathmin ribozyme expression can inhibit tumorigenicity of prostate cancer cells *in vitro*.

#### Effects of Anti-Stathmin Ribozyme on Apoptosis

In the cell proliferation assays described above, we observed massive cell death by trypan blue staining 5 days after infection with anti-stathmin adenoviruses. To investigate these observations further, we assessed the effects of anti-stathmin ribozymes on apoptosis of LNCaP cells (Fig. 6). We first evaluated the effects of anti-stathmin ribozymes on the morphology of the nuclei by 4',6-diamidino-2-phenylindole staining. Figure 6A illustrates nuclear chromatin condensation in cells transduced with ribozyme carrying adenoviruses. Nuclei of normal cells are stained homogeneously by 4',6-diamidino-2-phenylindole, whereas nuclei of apoptotic cells are highly irregular as a result of chromatin condensation. Infection of cells with Ad.Rz184.GFP or Ad.Rz305.GFP resulted in apoptosis in 29% and 25% of cells, respectively, compared with 0.6% in uninfected cells and 1% in cells infected with the control Ad.GFP virus (Fig. 6A). We also investigated the effects of anti-stathmin ribozymes on the activation of caspase-3. Uninfected cells and cells infected with either Ad.GFP, Ad.Rz184.GFP, or Ad.Rz305.GFP were stained with anti-caspase-3 antibody and analyzed by flow cytometry. Cells infected with control Ad.GFP showed no significant caspase-3 activation (1.6%). In contrast, caspase-3 activation was seen in 43% and 37% of cells infected with Ad.Rz184.GFP and Ad.Rz305.GFP, respectively (Fig. 6B). We also assessed the effects of anti-stathmin ribozymes on DNA fragmentation in a flow cytometric TUNEL assay. Cells infected with control Ad.GFP showed virtually no TUNEL-positive cells (1.3%), whereas cells infected with

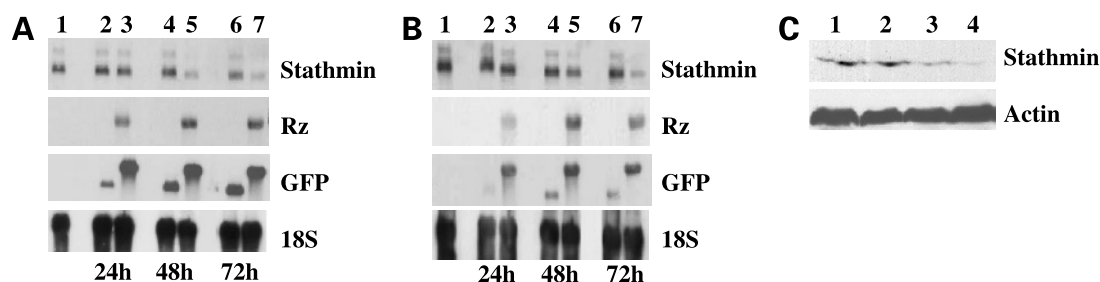


**Figure 2.** Kinetics of anti-stathmin ribozyme expression and activity in LNCaP cells. Total RNA was isolated from uninfected cells or cells infected with either Ad.GFP, Ad.Rz184.GFP, or Ad.Rz305.GFP at a MOI of 25. **A**, effects of Ad.Rz305.GFP on the level of stathmin mRNA. Lane 1, RNA (20  $\mu$ g) isolated from uninfected cells; lanes 2 to 7, RNA (20  $\mu$ g) isolated from cells transduced with Ad.GFP and Ad.Rz305.GFP at 24 h (lanes 2 and 3), 48 h (lanes 4 and 5), and 72 h (lanes 6 and 7). **B**, effects of Ad.Rz184.GFP on the level of stathmin mRNA. Lane 1, RNA (20  $\mu$ g) isolated from uninfected cells; lanes 2 to 7, RNA (20  $\mu$ g) isolated from cells transduced with Ad.GFP and Ad.Rz184.GFP at 24 h (lanes 2 and 3), 48 h (lanes 4 and 5), and 72 h (lanes 6 and 7). The filters were hybridized with stathmin, ribozyme (Rz), GFP, and 18S probes as indicated. **C**, effects of anti-stathmin adenoviruses on stathmin protein levels. Lanes 1 to 4, protein extracts (25  $\mu$ g) isolated from uninfected, Ad.GFP-infected, Ad.Rz305.GFP-infected, and Ad.Rz184.GFP-infected cells, respectively.

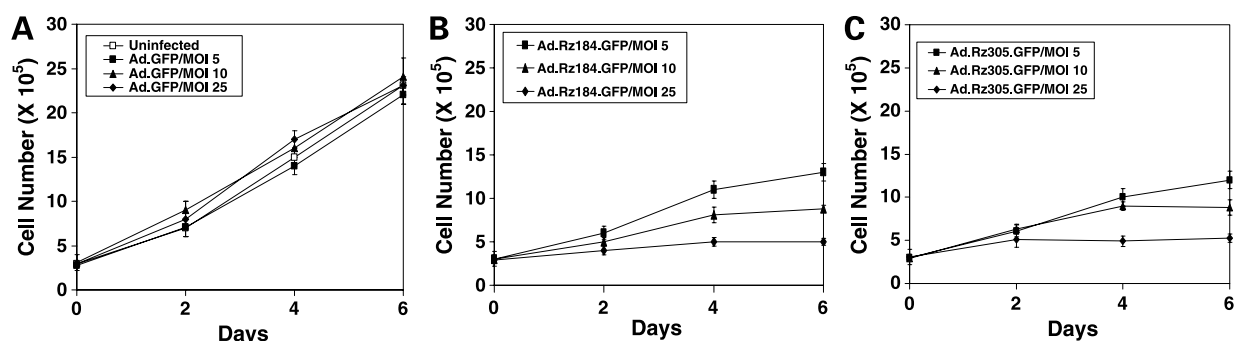


**Figure 3.** Effects of anti-stathmin ribozymes on the proliferation of LNCaP cells. **A**, growth curves of cells transduced with the control Ad.GFP adenovirus at different MOIs as indicated. **B**, growth curves of cells transduced with Ad.Rz184.GFP adenovirus at different MOIs as indicated. **C**, growth curves of cells transduced with Ad.Rz305.GFP adenovirus at different MOIs as indicated. Representative of three different experiments. Bars, SD.

Ad.Rz184.GFP and Ad.Rz305.GFP showed 59% and 56% TUNEL-positive cells, respectively (Fig. 6C). Thus, in all three assays, infection with adenoviral vectors that carry anti-stathmin ribozyme genes results in profound increase in apoptosis.

## Discussion

Prostate cancer is the most frequently diagnosed malignancy and the second leading cause of cancer-related deaths in men in the United States. In the early stage of the disease, the treatments of choice are extensive surgery

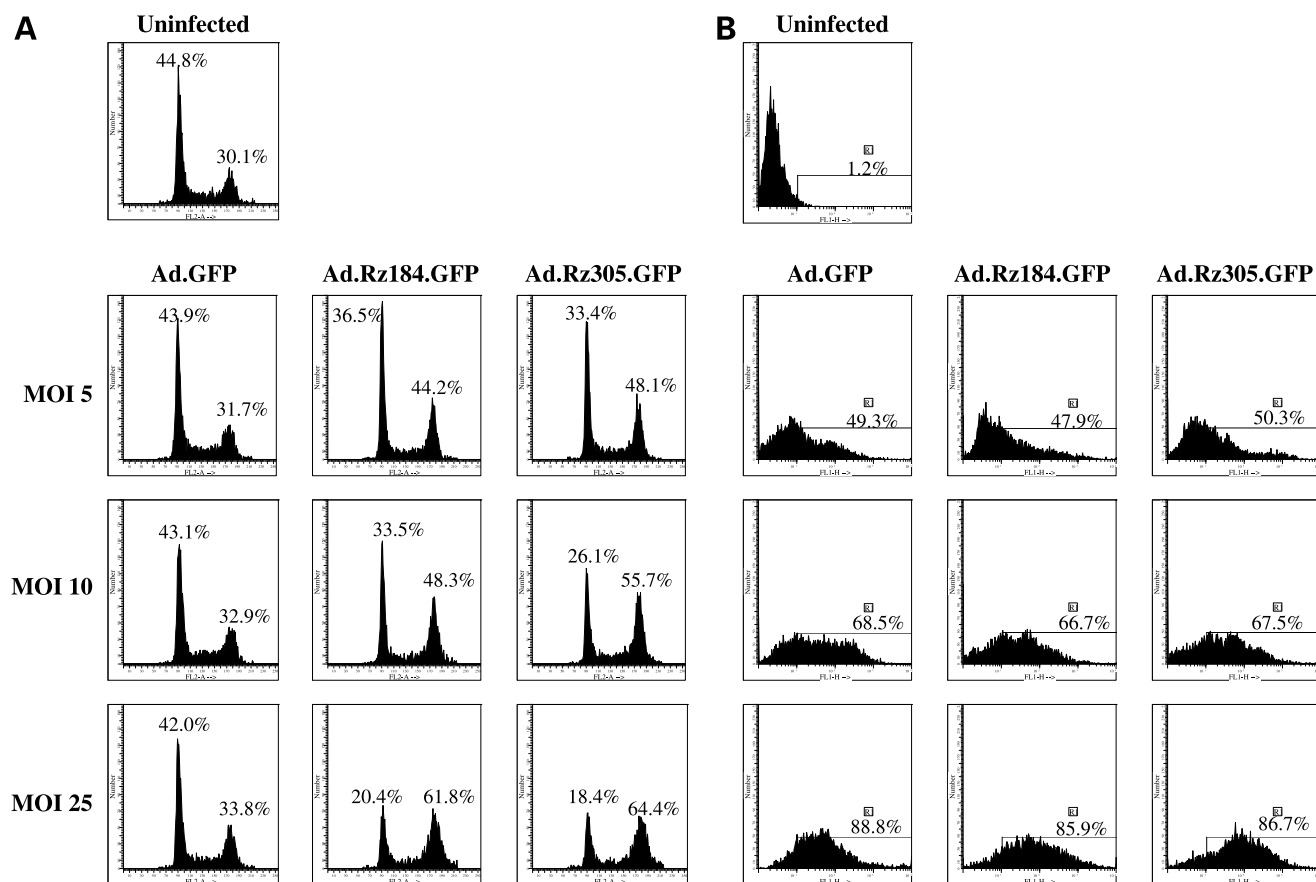


**Figure 4.** Effects of anti-stathmin ribozymes on cell cycle progression of LNCaP cells. **A**, DNA histograms of uninfected cells or cells infected with either Ad.GFP, Ad.Rz184.GFP, or Ad.Rz305.GFP as indicated. **B**, GFP fluorescence analysis of uninfected cells or cells infected with either Ad.GFP, Ad.Rz184.GFP, or Ad.Rz305.GFP as indicated. R1, the gate for GFP-positive cells.

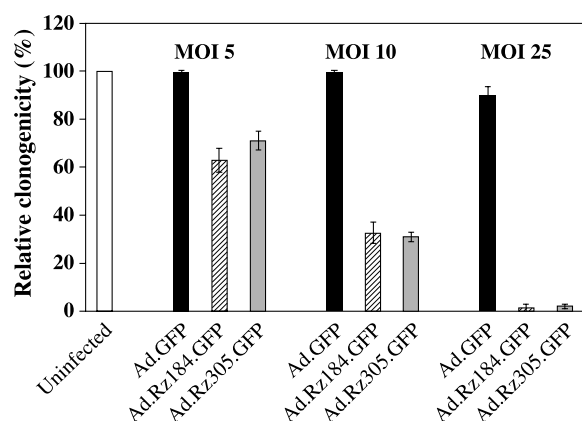


**Figure 5.** Effects of anti-stathmin ribozymes on the clonogenic potential of LNCaP cells. Clonogenic potential of uninfected cells or cells infected with either Ad.GFP, Ad.Rz184.GFP, or Ad.Rz305.GFP at different MOIs. The relative clonogenicity of infected cells was calculated relative to a clonogenic potential of uninfected cells of 100%. *Open column*, uninfected cells; *filled columns*, Ad.GFP-infected cells; *hatched columns*, Ad.Rz184.GFP-infected cells; *gray columns*, Ad.Rz305.GFP-infected cells. Representative of three different experiments. *Bars*, SD.

and/or radiation therapy. Although both treatment modalities are highly effective, they are associated with significant morbidity and mortality. The localized aspect of the disease in its early stages and its responsiveness to local therapy makes prostate cancer an attractive model for the development of a stathmin-based local therapy that might avoid the morbidity and mortality of extensive surgery and radiation therapy. When local therapies for prostate cancer fail and the disease progresses, systemic androgen ablation therapy, with or without chemotherapy, can frequently lead to tumor regression. However, the disease inevitably progresses to an androgen-independent state that is resistant to hormonal therapy and chemotherapy. Thus, the development of alternative therapeutic strategies for prostate cancer in the early and late stages remains a high priority. The aim of the studies described in this report is to develop a novel therapeutic strategy for the treatment of prostate cancer that targets the microtubules that make up the mitotic spindle.

Adenoviruses are efficient gene delivery vectors that are widely used in cancer gene therapy (26). They can be produced at very high titers and can infect a variety of cell types both *in vitro* and *in vivo* (26). Whereas retrovirus-mediated gene transfer results in stable integration of the transgene in transduced cells, adenoviruses do not integrate in the host genome (27). Moreover, adenoviruses induce an immune response in the host that can result in the clearance of transduced cells within 1 or 2 weeks after gene transfer (27). Although such an immune response is a major limitation in the gene therapy of genetic disease, it may be advantageous in cancer gene therapy because elimination of the transduced cells is an end point of therapy. Thus, we developed adenoviral gene transfer vectors to achieve efficient delivery of anti-stathmin ribozymes into prostate cancer cells. The experiments described above

show that the two anti-stathmin ribozymes that we described previously can be used in adenoviral gene transfer vectors to achieve very effective down-regulation of stathmin expression in prostate cancer cells. The progressive increase in ribozyme expression correlated with a corresponding decrease in the levels of stathmin mRNA and protein.

We investigated the therapeutic potential of adenovirus-mediated anti-stathmin therapy in several biological assays. Cell cycle analysis of anti-stathmin ribozyme-infected cells

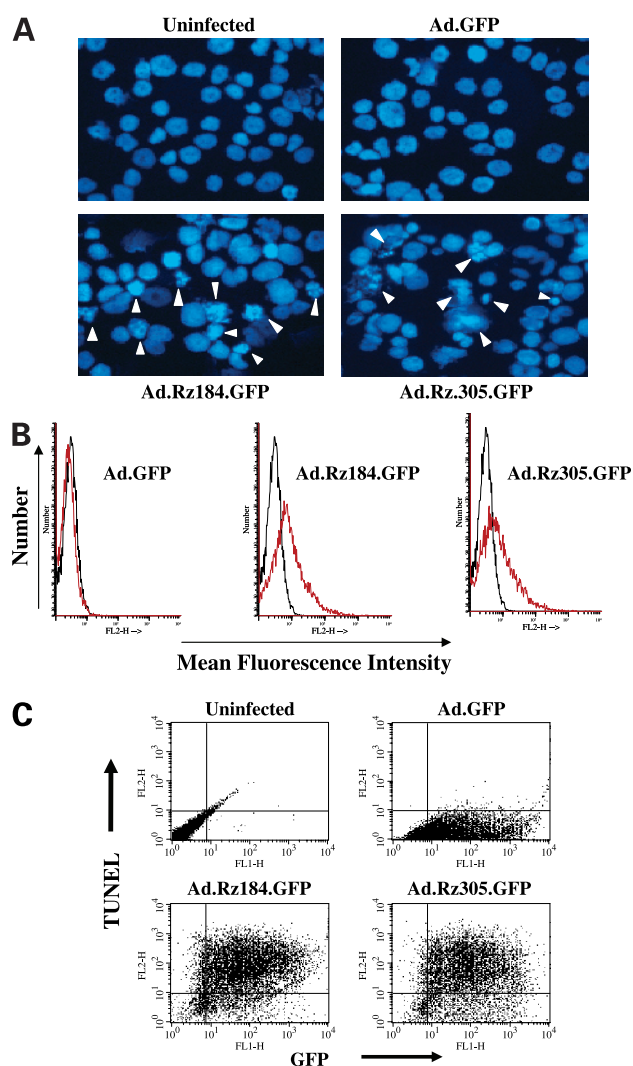


**Figure 6.** Effects of anti-stathmin ribozymes on apoptosis in LNCaP cells. **A**, nuclear morphology of uninfected and infected cells as indicated. Apoptotic nuclei (arrowheads) show characteristic chromatin condensation and nuclear fragmentation in anti-stathmin adenovirus infected cells after 4',6-diamidino-2-phenylindole staining. **B**, flow cytometric histograms showing the expression of caspase-3 in uninfected and infected cells as indicated. The uninfected cells were essentially negative for the presence of active caspase-3. The histogram of uninfected cells (black) is overlaid on histograms of Ad.GFP, Ad.Rz184.GFP, or Ad.Rz305.GFP (red) as indicated. **C**, DNA histograms showing the percentage of TUNEL-positive cells in uninfected, Ad.GFP-infected, Ad.Rz184.GFP-infected, and Ad.Rz305.GFP-infected cells as indicated.

showed a marked accumulation of cells in the G<sub>2</sub>-M phases of the cell cycle. These observations in prostate cancer cells are similar to previous observations that we and others made in leukemic cells (6, 7). Because stathmin is a catastrophe factor and/or sequesterer of tubulin that leads to depolymerization of microtubules (3, 4), inhibition of stathmin is expected to impede progression through mitosis. The mitotic block that we observed correlated with a dose-dependent inhibition of growth of LNCaP prostate cancer cells infected with the anti-stathmin adenoviruses. Similar antimitotic and antiproliferative effects were also observed in DU145 and PC3 prostate cancer cell lines (data not shown). The inclusion of the *GFP* gene in our adenoviral vectors allowed us to exclude the possibility that differences in the efficiency of transduction or cytotoxicity of the adenovirus itself may be the cause of the observed differences in proliferation and cell cycle progression.

Of all the *in vitro* assays of transformation, clonogenic anchorage-independent growth has the best correlation with *in vivo* assays of tumorigenicity (28, 29). Whereas nontransformed cells may divide once or twice in semisolid medium, transformed cells continue to divide until they form visible colonies. Using this assay, we showed that adenovirus-mediated anti-stathmin therapy results in a profound dose-dependent inhibition of the clonogenic growth of LNCaP cells. Interestingly, the reduced number of colonies that formed at lower MOIs in cells transduced with the anti-stathmin ribozymes were also much smaller compared with colonies that formed in uninfected or Ad.GFP-infected cells. Moreover, no further increase in the number or size of colonies was observed after 4 weeks in semisolid medium. We also assessed the effect of anti-stathmin ribozyme genes on apoptosis in LNCaP cells by analyzing cell morphology, caspase activation, and DNA fragmentation. Stathmin inhibition was associated with a marked increase in rounding and detachment of cells, increase in chromatin condensation, activation of caspase-3, and fragmentation of internucleosomal DNA. Although the increase in caspase-3 activation suggests that the apoptosis that we observed is induced by a caspase-dependent pathway, it is not clear what the exact mechanism of apoptosis is in those cells. We speculate that the mitotic spindle abnormalities that result from down-regulation of stathmin expression might activate mitotic checkpoints that lead to apoptosis.

Prostate cancer is generally considered a chemotherapy-resistant disease. Taxol is one of few chemotherapeutic agents that have activity against prostate cancer (30). The taxanes are a family of mitotic inhibitors that exert their antitumor effects by stabilizing the microtubules that make up the mitotic spindle (30). Although taxol has marked activity against prostate cancer cells *in vitro*, the results of clinical studies in which taxol was used as a single agent in prostate cancer have been disappointing (31, 32). Our previous studies have shown synergy between stathmin inhibition and taxol exposure in leukemic cells (33). If similar synergy is shown in prostate cancer cells that are

inherently more sensitive to taxol than leukemic cells, combination therapy consisting of taxol and anti-stathmin ribozymes may provide a potentially effective therapeutic approach for prostate cancer.

## Acknowledgments

We thank Dr. Anna Ferrari for the generous gift of LNCaP cell line.

## References

- Desai A, Mitchison TJ. Microtubule polymerization dynamics. *Annu Rev Cell Dev Biol* 1997;13:83–117.
- Andersen SS. Spindle assembly and the art of regulating microtubule dynamics by MAPs and stathmin/Op18. *Trends Cell Biol* 2000;10:261–7.
- Marklund U, Larsson N, Gradin HM, Brattsand G, Gullberg M. Oncoprotein 18 is a phosphorylation-responsive regulator of microtubule dynamics. *EMBO J* 1996;15:5290–8.
- Mistry SJ, Atweh GF. Stathmin inhibition enhances okadaic acid-induced mitotic arrest: a potential role for stathmin in mitotic exit. *J Biol Chem* 2001;276:31209–15.
- Horwitz SB, Shen HJ, He L, Dittmar P, et al. The microtubule-destabilizing activity of metastastin (p19) is controlled by phosphorylation. *J Biol Chem* 1997;272:8129–32.
- Luo XN, Mookerjee B, Ferrari A, Mistry S, Atweh GF. Regulation of phosphoprotein p18 in leukemic cells. Cell cycle regulated phosphorylation by p34cdc2 kinase. *J Biol Chem* 1994;269:10312–8.
- Marklund U, Osterman O, Melander H, Bergh A, Gullberg M. The phenotype of a “Cdc2 kinase target site-deficient” mutant of oncoprotein 18 reveals a role of this protein in cell cycle control. *J Biol Chem* 1994;269:30626–35.
- Hanash SM, Strahler J, Kuick R, Chu EHY, Nichols D. Identification of a polypeptide associated with the malignant phenotype in acute leukemia. *J Biol Chem* 1988;263:12813–5.
- Roos G, Brattsand G, Landberg G, Marklund U, Gullberg M. Expression of oncoprotein 18 in human leukemias and lymphomas. *Leukemia* 1993;7:1538–46.
- Hailat N, Strahler J, Melhem R, et al. N-myc gene amplification in neuroblastoma is associated with altered phosphorylation of a proliferation related polypeptide (Op18). *Oncogene* 1990;5:1615–8.
- Price DK, Ball JR, Bahrani-Mostafavi Z, et al. The phosphoprotein Op18/stathmin is differentially expressed in ovarian cancer. *Cancer Invest* 2000;18:722–30.
- Friedrich B, Gronberg H, Landstrom M, Gullberg M, Bergh A. Differentiation-stage specific expression of oncoprotein 18 in human and rat prostatic adenocarcinoma. *Prostate* 1995;27:102–9.
- Brattsand G. Correlation of oncoprotein 18/stathmin expression in human breast cancer with established prognostic factors. *Br J Cancer* 2000;83:311–8.
- Bieche I, Lachkar S, Becette V, et al. Overexpression of the stathmin gene in a subset of human breast cancer. *Br J Cancer* 1998;78:701–9.
- Brattsand G, Roos G, Marklund U, et al. Quantitative analysis of the expression and regulation of an activation-regulated phosphoprotein (oncoprotein 18) in normal and neoplastic cells. *Leukemia* 1993;7:569–79.
- Jeha S, Luo XN, Beran M, Kantarjian H, Atweh GF. Antisense RNA inhibition of phosphoprotein p18 expression abrogates the transformed phenotype of leukemic cells. *Cancer Res* 1996;56:1445–50.
- Mistry SJ, Benham CJ, Atweh GF. Development of ribozymes that target stathmin, a major regulator of the mitotic spindle. *Antisense Nucleic Acid Drug Dev* 2001;11:41–9.
- Irie A, Bouffard DY, Scanlon KJ. Ribozyme-mediated cancer gene therapy. *Int J Urol* 1997;4:329–37.
- Kijima H, Ishida H, Ohkawa T, Kashani-Sabet M, Scanlon KJ. Therapeutic applications of ribozymes. *Pharmacol Ther* 1995;68:247–67.
- Gao M, Ossowski L, Ferrari AC. Activation of Rb and decline in androgen receptor protein precede retinoic acid-induced apoptosis in androgen-dependent LNCaP cells and their androgen-independent derivative. *J Cell Physiol* 1999;179:336–46.
- Graham FL, Prevec L. Methods for construction of adenovirus vectors. *Mol Biotechnol* 1995;3:207–20.

22. Sambrook J, Fritsch EF, Maniatis T. Molecular cloning: a laboratory manual. 2nd ed. Cold Spring Harbor (NY): Cold Spring Harbor Laboratory; 1989.
23. Zhu XX, Kozarsky K, Strahler JR, et al. Molecular cloning of a novel human leukemia-associated gene. Evidence of conservation in animal species. *J Biol Chem* 1989;264:14556–60.
24. Gurtu V, Yan G, Zhang G. IRES bicistronic expression vectors for efficient creation of stable mammalian cell lines. *Biochem Biophys Res Commun* 1996;229:295–8.
25. Horoszewicz J, Leong S, Chu T, et al. The LNCaP cell line: a new model for studies on human prostatic carcinoma. *Prog Clin Biol Res* 1980;37:115–32.
26. Bramson JL, Graham FL, Gaudie J. The use of adenoviral vectors for gene therapy and gene transfer *in vivo*. *Curr Opin Biotechnol* 1995;6:590–5.
27. Leber SM, Masahito Y, Sanes JR. Gene transfer using replication-defective retroviral and adenoviral vectors. *Methods Cell Biol* 1996;51:161–83.
28. Shin SI, Freedman VH, Risser R, Pollack R. Tumorigenicity of virus-transformed cells in nude mice is correlated specifically with anchorage independent growth *in vitro*. *Proc Natl Acad Sci U S A* 1975;72:4435–9.
29. Freedman VH, Shin SI. Cellular tumorigenicity in nude mice correlates with cell growth in semi-solid medium. *Cell* 1974;3:355–9.
30. Stein CA. Mechanisms of action of taxanes in prostate cancer. *Semin Oncol* 1999;26:3–7.
31. Roth BJ, Yeap BY, Wilding G, Kasimis B, McLeod D, Loehrer PJ. Taxol in advanced, hormone-refractory carcinoma of the prostate: a phase II trial of the Eastern Cooperative Oncology Group. *Cancer* 1993;72:2457–60.
32. Kang MH, Figg WD, Dahut W. Taxanes in hormone-refractory prostate cancer. *Cancer Pract* 1999;7:270–2.
33. Iancu C, Mistry SJ, Arkin S, Atweh GF. Taxol and anti-stathmin therapy: a synergistic combination that targets the mitotic spindle. *Cancer Res* 2000;60:3537–41.

# Therapeutic interactions between stathmin inhibition and chemotherapeutic agents in prostate cancer

Sucharita J. Mistry and George F. Atweh

Division of Hematology-Oncology, Department of Medicine,  
Mount Sinai School of Medicine, New York, New York

## Abstract

Limitations of prostate cancer therapy may be overcome by combinations of chemotherapeutic agents with gene therapy directed against specific proteins critical for disease progression. Stathmin is overexpressed in many types of human cancer, including prostate cancer. Stathmin is one of the key regulators of the microtubule network and the mitotic spindle and provides an attractive therapeutic target in cancer therapy. We recently showed that adenovirus-mediated gene transfer of anti-stathmin ribozyme could suppress the malignant phenotype of prostate cancer cells *in vitro*. In the current studies, we asked whether the therapeutic effects of stathmin inhibition could be further enhanced by exposure to different chemotherapeutic agents. Exposure of uninfected LNCaP human prostate cancer cells or cells infected with a control adenovirus to Taxol, etoposide, 5-fluorouracil (5-FU), or Adriamycin resulted in modest decrease in proliferation and clonogenicity. Interestingly, exposure of cells infected with an anti-stathmin adenovirus to Taxol or etoposide resulted in a complete loss of proliferation and clonogenicity, whereas exposure of the same cells to 5-FU or Adriamycin potentiated the growth-inhibitory effects of the anti-stathmin ribozyme, but the cells continued to proliferate. Terminal deoxynucleotidyl transferase-mediated dUTP nick end labeling analysis of uninfected cells or cells infected with a control adenovirus showed modest induction of apoptosis in the presence of different drugs. In contrast, cells infected with the anti-stathmin adenovirus showed a marked increase in apoptosis on exposure to Taxol or etoposide and a modest increase on exposure to 5-FU or Adriamycin. Overall, the effects of

combinations of anti-stathmin ribozyme with Taxol or etoposide were synergistic, whereas the effects of combinations of anti-stathmin ribozyme with 5-FU or Adriamycin were additive. Moreover, triple combination of anti-stathmin ribozyme with low noninhibitory concentrations of Taxol and etoposide resulted in a profound synergistic inhibition of proliferation, clonogenicity, and marked induction of apoptosis. This synergy might be very relevant for the treatment of prostate cancer because Taxol and etoposide are two of the most effective agents in this disease. Thus, this combination may provide a novel form of prostate cancer therapy that would avoid toxicities associated with the use of multiple chemotherapeutic agents at full therapeutic doses. [Mol Cancer Ther 2006;5(12):3248–57]

## Introduction

Prostate cancer is the most frequently diagnosed malignancy and the second leading cause of cancer-related deaths among men in the United States. In the early stage of the disease, the treatments of choice are radical surgery or radiation therapy. Both treatment modalities are associated with significant morbidity and mortality. Although, in advanced prostate cancer, systemic androgen ablation frequently leads to tumor regression, the disease usually progresses to an androgen-independent state that does not respond to endocrine manipulations. Although chemotherapy can have some therapeutic benefits, prostate cancer is widely viewed as a chemoresistant neoplasm. Thus, novel therapeutic approaches are needed to improve the outlook for patients with advanced prostate cancer.

Stathmin is the founding member of a family of microtubule-destabilizing proteins that play a critically important role in the assembly and disassembly of the mitotic spindle (1–4). It regulates the mitotic spindle through cell cycle-dependent changes in its state of phosphorylation that are mediated by p34<sup>cdc2</sup> kinase, mitogen-activated protein kinase, and other kinases (2, 5–8). Stathmin is expressed at high levels in a wide variety of human malignancies, including prostate carcinoma (9–12), and provides an attractive target for cancer therapy (13). High levels of stathmin expression in cancer cells were shown to correlate with their proliferative potential and seem to be necessary for the maintenance of their malignant phenotype (13–15). Interestingly, when biopsy specimens from human prostate cancers were immunostained with an anti-stathmin antibody, immunoreactivity was seen in poorly differentiated tumors but not in hyperplastic prostate or highly differentiated tumors (12). More importantly, the level of expression of stathmin was shown to correlate with the malignant behavior of prostate cancer (12). Hence, it was proposed

Received 4/27/06; revised 8/24/06; accepted 10/25/06.

**Grant support:** Department of Defense Research grants W81XWH-04-1-0219 (G.F. Atweh) and W81XWH-04-1-0673 (S.J. Mistry).

The costs of publication of this article were defrayed in part by the payment of page charges. This article must therefore be hereby marked advertisement in accordance with 18 U.S.C. Section 1734 solely to indicate this fact.

**Requests for reprints:** Sucharita J. Mistry, Division of Hematology-Oncology, Department of Medicine, Mount Sinai School of Medicine, One Gustave L. Levy Place, Box 1079, New York, NY 10029. Phone: 212-241-5281. E-mail: sucharita.mistry@mssm.edu or George F. Atweh, Division of Hematology-Oncology, Department of Medicine, Mount Sinai School of Medicine, One Gustave L. Levy Place, Box 1079, New York, NY 10029. Phone: 212-241-5293. E-mail: george.atweh@mssm.edu

Copyright © 2006 American Association for Cancer Research.

doi:10.1158/1535-7163.MCT-06-0227

that the level of expression of stathmin may serve as a prognostic marker in prostate cancer (12).

We recently generated replication-deficient bicistronic adenoviral vectors that carry an anti-stathmin ribozyme that targets stathmin mRNA in prostate cancer cells (16, 17). We showed that adenovirus-mediated gene transfer of anti-stathmin ribozyme can suppress the malignant phenotype of prostate cancer cells *in vitro* (17). In this study, we asked whether the therapeutic effects of anti-stathmin ribozyme in prostate cancer could be further enhanced by exposure to chemotherapeutic agents. Thus, we evaluated the effects of combinations of anti-stathmin adenovirus with four different chemotherapeutic agents on proliferation, clonogenicity, and apoptosis in human prostate cancer cells.

## Materials and Methods

### Reagents

Taxol (paclitaxel), etoposide, 5-fluorouracil (5-FU), and Adriamycin were purchased from Sigma (St. Louis, MO). All four drugs were dissolved in DMSO as a 10 mmol/L stock solution and stored at  $-20^{\circ}\text{C}$  in aliquots.

### Cell Lines

The human androgen-independent LNCaP prostate cancer cell line that we used in this study was described previously (18). LNCaP cells were grown in RPMI 1640 supplemented with 10% charcoal-stripped fetal bovine serum, 5  $\mu\text{g}/\text{mL}$  human insulin, 100 units/mL penicillin, and 100  $\mu\text{g}/\text{mL}$  streptomycin. The cells were maintained at  $37^{\circ}\text{C}$  in a humidified 5%  $\text{CO}_2$  environment.

### Production of Recombinant Adenoviruses

The recombinant adenoviruses that we used in this study were previously described in detail (17). Briefly, a replication-deficient bicistronic adenoviral vector (Ad.Rz.GFP) that coexpresses green fluorescent protein (GFP) and an anti-stathmin ribozyme (Rz305) was constructed for targeting human stathmin mRNA (16, 17). The control vector contained the GFP reporter gene under the control of the CMV5 promoter without the anti-stathmin ribozyme sequences (17). Each recombinant transfer plasmid was cotransfected with part of the Ad5 genome selected to promote *in vivo* homologous recombination between the two DNA molecules, resulting in infectious adenoviruses. The recombinant adenoviruses were propagated in 293 cells, purified by cesium chloride gradient ultracentrifugation, dialyzed, and stored at  $-80^{\circ}\text{C}$  (17, 19). The infectious viral titers were determined by plaque assays in 293 cells (17, 19).

### Adenoviral Infections *In vitro*

Cells were seeded in six-well culture plates 24 h before virus infection. For all experiments described below, cells were infected with either control Ad.GFP or anti-stathmin Ad.Rz.GFP adenoviruses at a multiplicity of infection (MOI) of 5 in 2% reduced serum medium for 3 h. After infection, the virus was removed and the cells were further incubated in complete growth medium. The efficiency of transduction by the recombinant adenoviruses was confirmed by measuring the fraction of cells that expressed GFP by flow cytometry or fluorescence microscopy as described previously (17).

### Cell Proliferation Assays

To assess the rate of proliferation, equal numbers of cells ( $2 \times 10^5$ ) were infected with either control or anti-stathmin adenoviruses in triplicates and the cells were exposed to different chemotherapeutic agents at various concentrations (Taxol, 1–6 nmol/L; etoposide, 0.5–2  $\mu\text{mol}/\text{L}$ ; 5-FU, 1–5  $\mu\text{mol}/\text{L}$ ; or Adriamycin, 2–10 nmol/L). The cells (floating and detached) were harvested and stained with trypan blue to determine cell viability. Viable cells were counted in a hemocytometer on alternate days, and growth curves were generated using the means of triplicate alternate day cell counts.

To assess the effects of triple combination of anti-stathmin ribozyme, Taxol, and etoposide, uninfected cells and cells infected with either Ad.GFP or Ad.Rz.GFP were incubated in the presence or absence of two different groups of noninhibitory concentrations of Taxol and etoposide: (a) 1 nmol/L Taxol and 0.25  $\mu\text{mol}/\text{L}$  etoposide or 1 nmol/L Taxol and 0.5  $\mu\text{mol}/\text{L}$  etoposide and (b) 2 nmol/L Taxol and 0.25  $\mu\text{mol}/\text{L}$  etoposide or 2 nmol/L Taxol and 0.5  $\mu\text{mol}/\text{L}$  etoposide. Cells were counted on alternate days, and growth curves were generated as above.

### Clonogenic Assays

Anchorage-independent growth was assessed by colony formation in a methylcellulose semisolid medium (17). Equal numbers of cells were infected with either control or anti-stathmin adenoviruses in triplicates as above, and the cells were incubated in growth medium containing different chemotherapeutic agents (Taxol, 4 nmol/L; etoposide, 2  $\mu\text{mol}/\text{L}$ ; 5-FU, 5  $\mu\text{mol}/\text{L}$ ; or Adriamycin, 10 nmol/L) for 3 days. The cells were then washed in PBS, and equal numbers of cells ( $1 \times 10^4$ ) were resuspended in 5 mL methylcellulose-based semisolid medium (0.9% methylcellulose, 1% bovine serum albumin, and 0.1 mmol/L  $\beta$ -mercaptoethanol prepared in RPMI 1640 containing 30% fetal bovine serum, 100 units/mL penicillin, and 100  $\mu\text{g}/\text{mL}$  streptomycin; ref. 17). The cells were plated in six-well tissue culture plates in triplicates and incubated at  $37^{\circ}\text{C}$  in 5%  $\text{CO}_2$ . The colonies that formed were counted after 2 weeks. For triple combination studies, uninfected cells or cells infected with either control Ad.GFP or Ad.Rz.GFP were incubated in growth medium with or without Taxol (1 nmol/L) and etoposide (0.5  $\mu\text{mol}/\text{L}$ ) for 3 days. The cells were plated in methylcellulose as above.

### Cell Cycle Analysis

We used propidium iodide staining of fixed whole cells to analyze the distribution of cells in the different phases of the cell cycle as described previously (17). LNCaP cells were infected either with control or anti-stathmin adenoviruses at a MOI of 5 as above. Three hours after infection, the virus was removed and the cells were incubated in growth medium without drugs or in growth medium containing 1 nmol/L Taxol and 0.5  $\mu\text{mol}/\text{L}$  etoposide. After 48 h, the cells were harvested, fixed in 70% ethanol, washed in PBS, and resuspended for 30 min at  $37^{\circ}\text{C}$  in 1 mL propidium iodide solution (PBS containing 0.05 mg/mL, 0.1% sodium citrate, and 1  $\mu\text{g}/\text{mL}$  RNase; ref. 17). DNA

content was analyzed within 2 h in a Becton Dickinson (Bedford, MA) FACStar Plus flow cytometer at 488-nm single laser excitation. The cell cycle distribution was analyzed using WinList software.

#### Evaluation of Therapeutic Interactions

The therapeutic interactions between the anti-stathmin adenovirus and the different drugs were analyzed according to the method of Chou and Talalay (20) with the help of the Calcsyn software suite (Biosoft, Cambridge, United Kingdom). Median effect plots were determined by generating dose-response curves for anti-stathmin adenovirus, Taxol, etoposide, Adriamycin, and 5-FU. Combination index (CI) values were then calculated at different drug concentrations, and the Fa-CI plots were generated by Calcsyn. According to Chou and Talalay, a CI of <1 indicates a synergistic interaction, a CI of 1 indicates an additive interaction, and a CI of >1 indicates an antagonistic interaction (20).

#### Apoptosis Assays

To evaluate the effects of the combinations of anti-stathmin ribozyme with different chemotherapeutic agents on apoptosis, we used terminal deoxynucleotidyl transferase-mediated dUTP nick end labeling (TUNEL) assay (17). Cells infected with either control or anti-stathmin adenoviruses were incubated in growth medium containing different chemotherapeutic agents (Taxol, 4 nmol/L; etoposide, 2  $\mu$ mol/L; 5-FU, 5  $\mu$ mol/L; or Adriamycin, 10 nmol/L).

Both floating and attached cells were harvested 5 days later, and the effect of ribozyme-mediated stathmin inhibition on apoptosis was quantified. DNA fragmentation was assessed by TUNEL assay using a cell death detection kit (Roche Applied Science, Indianapolis, IN) according to the instructions of the manufacturer. Briefly, the cells were fixed, permeabilized, and incubated with the TUNEL reaction mixture. The free 3' OH groups of fragmented DNA labeled with tetramethylrhodamine-labeled nucleotides were quantified by flow cytometry as described (17). For triple combination studies, cells infected with either Ad.GFP or Ad.Rz.GFP were incubated in the presence or absence of Taxol (1 nmol/L) and etoposide (0.5  $\mu$ mol/L) for 5 days and analyzed by the TUNEL assay as above.

#### Statistical Analysis

The data are expressed as mean  $\pm$  SD. The data were analyzed for statistical significance using the two-tailed Student's *t* test. *P*s < 0.05 were considered statistically significant.

## Results

We evaluated the effects of anti-stathmin ribozyme in combination with different chemotherapeutic drugs on the growth rates of LNCaP cells. Figure 1 illustrates the effects of different concentrations of four chemotherapeutic drugs

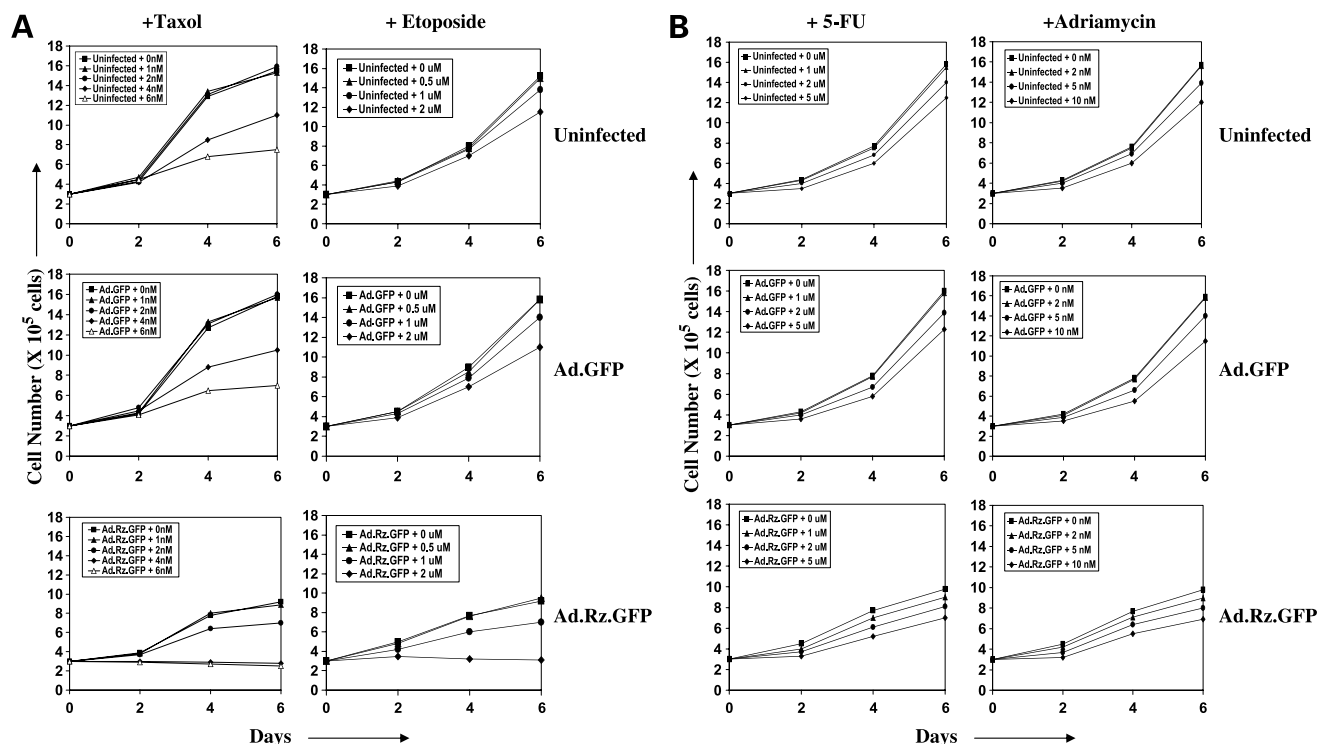


**Figure 1.** Effects of combination of chemotherapeutic agents and anti-stathmin adenovirus on the rate of proliferation of LNCaP cells. **A**, growth curves of uninfected cells and cells infected with either control Ad.GFP or Ad.Rz.GFP adenoviruses in the presence and absence of different concentrations of Taxol or etoposide. **B**, growth curves of uninfected cells and cells infected with either control Ad.GFP or Ad.Rz.GFP adenoviruses in the presence and absence of different concentrations of 5-FU or Adriamycin. Points, mean of triplicate alternate day cell counts.

on the rate of proliferation of LNCaP cells in the presence and absence of anti-stathmin ribozyme. Interactions between different therapeutic agents are best evaluated at low subtherapeutic concentrations to avoid saturation artifacts. In the experiment illustrated in Fig. 1, we used a low MOI of the recombinant adenoviruses (i.e., MOI of 5) and low concentrations of the different chemotherapeutic drugs. Transduction efficiencies in cells infected with the recombinant adenovirus ranged from 65% to 75% in the experiments described. The concentrations of the different drugs that we used were selected in pilot experiments and were significantly below the IC<sub>50</sub> (data not shown). The proliferative rates of uninfected cells or cells infected with the control Ad.GFP virus were not affected by the lower concentrations of Taxol (1–2 nmol/L) and were modestly inhibited at increasing concentrations of Taxol (4–6 nmol/L; Fig. 1A). Similarly, exposure of uninfected cells or cells infected with the control Ad.GFP virus to etoposide resulted in modest dose-dependent decrease in growth rates (Fig. 1A). In contrast, exposure of cells infected with Ad.Rz.GFP virus to the same concentrations of Taxol or etoposide resulted in marked growth inhibition at the lower concentrations and a virtually complete loss of proliferation at the higher concentrations of Taxol or etoposide (Fig. 1A). Exposure of cells to different concentrations of 5-FU (1–5  $\mu$ mol/L) or Adriamycin (2–10 nmol/L) also resulted in a modest dose-dependent decrease in proliferation of uninfected cells and cells infected with the control Ad.GFP virus (Fig. 1B). Although exposure of Ad.Rz.GFP-infected cells to 5-FU or Adriamycin resulted in further growth inhibition, the cells continued to proliferate (Fig. 1B). Thus, stathmin inhibition seemed to result in greater sensitization of prostate cancer cells to the growth-inhibitory effects of Taxol and etoposide than to those of 5-FU or Adriamycin.

We also evaluated the effects of the combinations of anti-stathmin ribozyme with different chemotherapeutic agents on apoptosis in LNCaP cells (Fig. 2). TUNEL analysis of cells infected with the control Ad.GFP adenovirus showed very little apoptosis (0.4%; Fig. 2A). When the control Ad.GFP-infected cells were exposed to Taxol, etoposide, Adriamycin, or 5-FU, the fraction of TUNEL-positive cells increased modestly to 2.8%, 3.5%, 1.1%, and 1.7%, respectively (Fig. 2B–E). Infection of cells with Ad.Rz.GFP adenovirus alone at a low MOI resulted in a slightly larger fraction of TUNEL-positive cells (3.7%) than in cells infected with the control Ad.GFP virus (0.4%; Fig. 2A). The fraction of TUNEL-positive cells were also slightly higher when Ad.Rz.GFP-infected cells were exposed to Adriamycin and 5-FU (6.6% and 7.2%, respectively; Fig. 2D and E). However, a much larger increase in the fraction of apoptotic cells was observed when Ad.Rz.GFP-infected cells were exposed to Taxol (25.8%) or etoposide (22.2%; Fig. 2A and B). Thus, when anti-stathmin adenovirus is used in combination with chemotherapeutic agents, a much larger increase in apoptosis was seen in the presence of etoposide and Taxol than in the presence of Adriamycin and 5-FU.

We then examined the effects of combinations of anti-stathmin ribozyme with different chemotherapeutic agents on the clonogenic potential of LNCaP cells. The clonogenic assay is the *in vitro* assay that correlates best with *in vivo* assays of tumorigenicity (21, 22). Figure 3 illustrates the effects of combinations of Ad.GFP or Ad.Rz.GFP adenoviruses with different drugs on the clonogenicity of LNCaP cells. Clonogenicity of cells infected with the control Ad.GFP virus was reduced by 35%, 39%, 31%, and 32% on exposure to Taxol (Fig. 3B), etoposide (Fig. 3C), Adriamycin (Fig. 3D), and 5-FU (Fig. 3E), respectively.

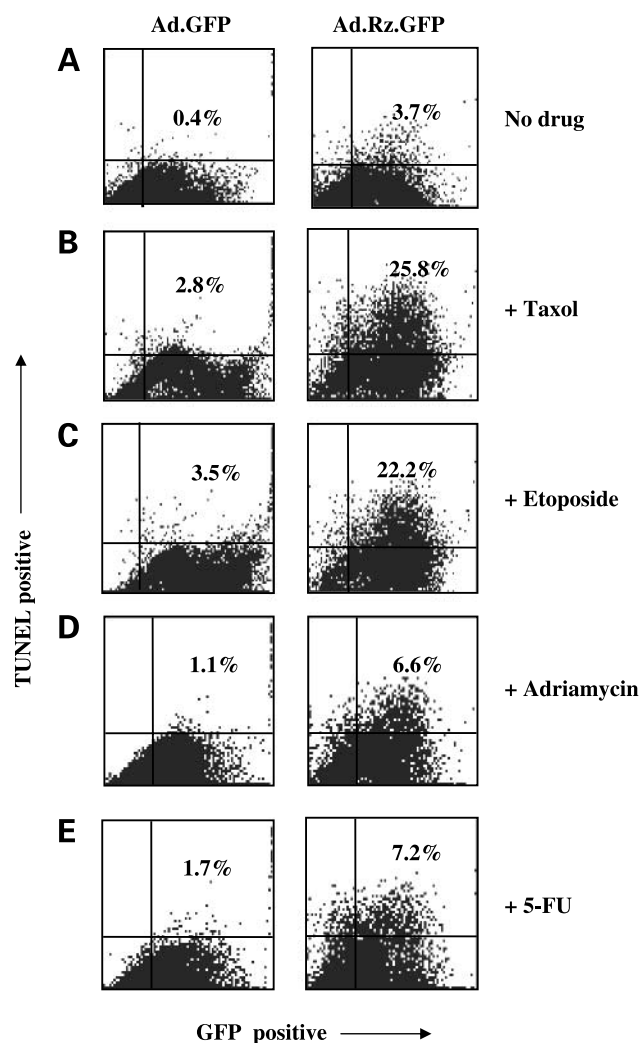


**Figure 2.** Effects of combination of Taxol and anti-stathmin adenovirus on apoptosis in LNCaP cells. **A**, dot plot showing the fraction of TUNEL positivity in Ad.GFP- and Ad.Rz.GFP-infected cells in the absence of the drugs. **B**, dot plot showing the fraction of TUNEL positivity in Ad.GFP- and Ad.Rz.GFP-infected cells after exposure to Taxol. **C**, dot plot showing the fraction of TUNEL positivity in Ad.GFP- and Ad.Rz.GFP-infected cells after exposure to etoposide. **D**, dot plot showing the fraction of TUNEL positivity in Ad.GFP- and Ad.Rz.GFP-infected cells after exposure to Adriamycin. **E**, dot plot showing the percentage of TUNEL positivity in Ad.GFP- and Ad.Rz.GFP-infected cells after exposure to 5-FU. The experiment is a representative of three independent experiments.

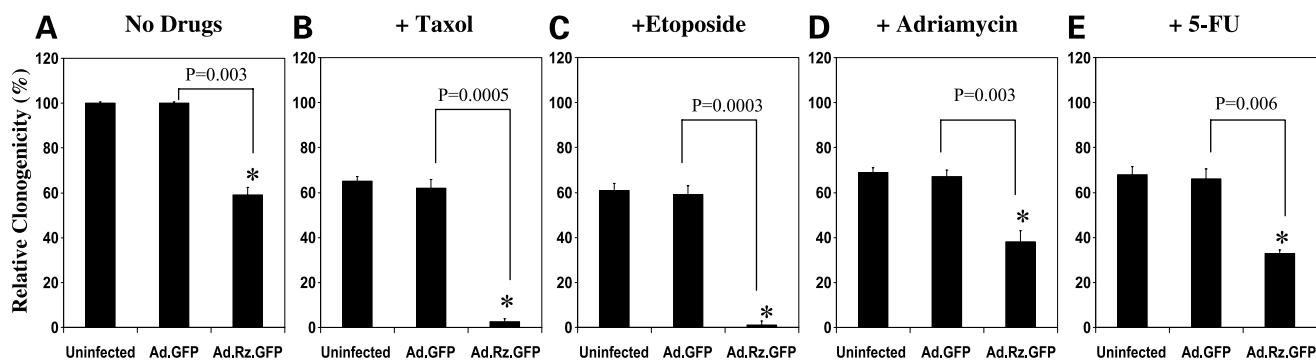


**Figure 3.** Effects of combination of anti-stathmin adenovirus and chemotherapeutic agents on the clonogenic potential of LNCaP cells. **A**, clonogenicity of uninfected, control Ad.GFP-infected, and Ad.Rz.GFP-infected cells at baseline in the absence of drug exposure. **B**, effect of combination of anti-stathmin ribozyme and Taxol exposure on the clonogenicity of uninfected, control Ad.GFP-infected, and Ad.Rz.GFP-infected cells. **C**, effect of combination of anti-stathmin ribozyme and etoposide exposure on the clonogenicity of uninfected, control Ad.GFP-infected, and Ad.Rz.GFP-infected cells. **D**, effect of combination of anti-stathmin ribozyme and Adriamycin exposure on the clonogenicity of uninfected, control Ad.GFP-infected, and Ad.Rz.GFP-infected cells. **E**, effect of combination of anti-stathmin ribozyme and 5-FU exposure on the clonogenicity of uninfected, control Ad.GFP-infected, and Ad.Rz.GFP-infected cells. Columns, mean of three different experiments; bars, SD. Statistical significance was determined using Student's *t* test. Asterisks, statistically significant inhibition of clonogenicity.

The decrease in the clonogenic potential of Ad.GFP-infected cells on exposure to the same drugs was similar to that seen in uninfected cells (Fig. 3B–E). Moreover, stathmin inhibition alone resulted in a 42% decrease in clonogenicity in Ad.Rz.GFP-infected cells relative to control Ad.GFP-infected cells ( $P = 0.003$ ; Fig. 3A). When Ad.Rz.GFP-infected cells were exposed to Taxol or etoposide, clonogenicity was profoundly decreased by 96% ( $P = 0.0005$ ; Fig. 3B) and 98% ( $P = 0.0003$ ; Fig. 3C), respectively. In comparison, clonogenicity of the same cells was only moderately reduced to 40% ( $P = 0.006$ ) and 38% ( $P = 0.003$ ) on exposure to Adriamycin (Fig. 3D) or 5-FU (Fig. 3E). Thus, the observed decrease in clonogenicity following exposure to anti-stathmin adenovirus with Taxol (Fig. 3B) or etoposide (Fig. 3C) is much greater than the decrease in clonogenicity following exposure to anti-stathmin adenovirus with Adriamycin (Fig. 3D) or 5-FU (Fig. 3E). The same combinations were tested at different drug concentrations, and the observed anticlonogenic effects in Ad.Rz.GFP-infected cells were always more potent in cells exposed to Taxol or etoposide than in cells exposed to 5-FU or Adriamycin (data not shown).

We used the median effect analysis method of Chou and Talalay (20) to determine whether the observed effects on clonogenicity were additive or synergistic. This method identifies an interaction as synergistic, additive, or antagonistic by determining the difference between the observed combination effect and the expected additive effect. We used the CalcuSyn software that uses the equations of Chou and Talalay to assess the therapeutic interactions between the anti-stathmin adenovirus and different chemotherapeutic agents. This software takes into account both the potency ( $D_m$  values) and the shapes of the dose-effect curves ( $m$  values) to precisely analyze the combination effect of two agents. The CI values and the fraction affected (Fa) for each dose were used to generate the Fa-CI plots (Fig. 4). The CI values were determined to be  $<1$  when the

anti-stathmin adenovirus was combined with different concentrations of either Taxol (1–6 nmol/L; Fig. 4A) or etoposide (0.25–2  $\mu$ mol/L; Fig. 4B). In contrast, the CI values were  $\sim 1$  when the anti-stathmin adenovirus was combined with different concentrations of either Adriamycin (1–10 nmol/L; Fig. 4C) or 5-FU (0.5–5  $\mu$ mol/L; Fig. 4D). Thus, these data are indicative of a synergistic interaction when the anti-stathmin adenovirus is combined with either Taxol or etoposide and an additive interaction when the anti-stathmin adenovirus is combined with either Adriamycin or 5-FU.

Because taxanes and etoposide are frequently used together in combination therapy in prostate cancer, we tested the combination of anti-stathmin ribozyme with Taxol and etoposide on proliferation, clonogenicity, and apoptosis in LNCaP cells. In these studies, we used much lower concentrations of Taxol and etoposide that had no significant growth-inhibitory effects in uninfected cells or cells infected with the control Ad.GFP virus. These concentrations were also noninhibitory when used in cells infected with Ad.Rz.GFP adenovirus as shown in Fig. 1. Figure 5 illustrates the effects of the triple combination of anti-stathmin ribozyme, Taxol, and etoposide on the rate of proliferation of LNCaP cells. Exposure of uninfected cells or cells infected with control Ad.GFP virus to low noninhibitory concentrations of either Taxol (1 nmol/L) or etoposide (0.25 or 0.5  $\mu$ mol/L) resulted in a modest but reproducible decrease in the rate of proliferation (Fig. 5A). In contrast, exposure of Ad.Rz.GFP-infected cells to 1 nmol/L Taxol and 0.25  $\mu$ mol/L etoposide resulted in a more marked decrease in the rate of proliferation, whereas a complete loss of proliferation was observed at 1 nmol/L Taxol and 0.5  $\mu$ mol/L etoposide (Fig. 5A). When uninfected cells or cells infected with control Ad.GFP virus were exposed to higher but also noninhibitory concentrations (2 nmol/L Taxol and 0.25  $\mu$ mol/L etoposide or 2 nmol/L Taxol and 0.5  $\mu$ mol/L etoposide), there was a slight

increase in inhibition of proliferation (Fig. 5B). However, exposure of cells infected with Ad.Rz.GFP adenovirus to the same concentrations resulted in complete cessation of growth (Fig. 5B). Similarly, in *in vitro* clonogenic assays, the observed anticlonogenic effects in Ad.Rz.GFP-infected cells at different noninhibitory drug concentrations were always more potent than the effects of anti-stathmin ribozyme alone or the drugs alone. Figure 6 is a representative illustration of the effects of low noninhibitory concentrations of Taxol (1 nmol/L) and etoposide (0.5  $\mu$ mol/L) on the clonogenic potential of LNCaP cells in the presence and absence of stathmin inhibition. Clonogenicity of uninfected cells or cells infected with control Ad.GFP virus was modestly reduced by 20% following exposure to low concentrations of Taxol and etoposide (Fig. 6B) relative to the clonogenicity of the same cells in the absence of the drugs (Fig. 6A). In contrast, stathmin inhibition alone decreased the clonogenicity of the Ad.Rz.GFP-infected cells by 42% ( $P = 0.003$ ; Fig. 6A). More strikingly, when Ad.Rz.GFP-infected cells were exposed to Taxol and etoposide, clonogenicity was drastically reduced by >98% ( $P = 0.0006$ ; Fig. 6B).

To gain insights into the mechanism of synergistic inhibition of growth on exposure of LNCaP cells to anti-stathmin ribozyme, Taxol, and etoposide, we compared the cell cycle distribution of cells that were exposed to Taxol and etoposide in the presence and absence of stathmin inhibition (Fig. 7). Figure 7A shows the cell cycle distribution of uninfected cells, cells infected with the control Ad.GFP adenovirus, and cells infected with Ad.Rz.GFP adenovirus in the absence of the drugs. Exposure of uninfected cells or control Ad.GFP-infected cells to low noninhibitory concentrations of Taxol (1 nmol/L)

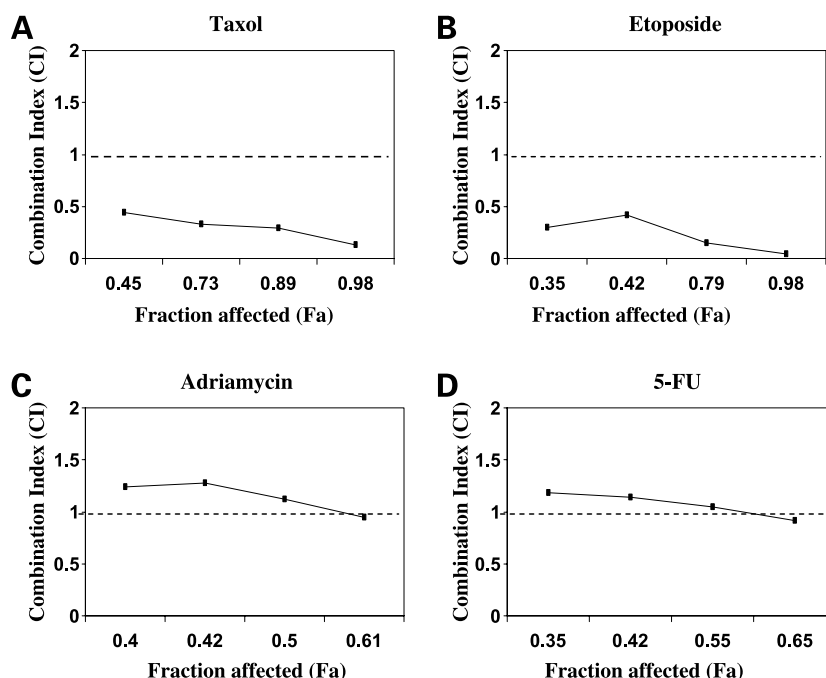
and etoposide (0.5  $\mu$ mol/L) resulted in a modest increase in accumulation of cells in the G<sub>2</sub>-M phases, with a corresponding decrease in the fraction of cells in the G<sub>0</sub>-G<sub>1</sub> phases of the cell cycle (Fig. 7B). In contrast, a much more profound mitotic arrest occurred when the cells were exposed to the same concentrations of Taxol and etoposide in the presence of stathmin inhibition (Fig. 7B).

We also analyzed the effects of the triple combination on apoptosis by TUNEL assay. The cells infected with the control Ad.GFP virus showed a very small fraction of TUNEL-positive cells (0.3%), whereas infection with the Ad.Rz.GFP virus resulted in slightly more TUNEL-positive cells (3.6%; Fig. 8A). After exposure to low noninhibitory concentrations of Taxol (1 nmol/L) and etoposide (0.5  $\mu$ mol/L), the fraction of TUNEL-positive cells in Ad.Rz.GFP-infected cells increased to 37.9% (Fig. 8B). Thus, in this assay too, exposure to low noninhibitory concentrations of Taxol and etoposide resulted in a much greater increase in the fraction of TUNEL positivity in cells infected with Ad.Rz.GFP adenovirus compared with uninfected cells or cells infected with the control Ad.GFP adenovirus (data not shown). Thus, stathmin inhibition can enhance the effects of very low concentrations of Taxol and etoposide to result in very potent inhibition of proliferation, clonogenicity, and marked induction of apoptosis.

## Discussion

Prostate cancer is generally considered a chemotherapy-insensitive disease. Conventional chemotherapy in advanced prostate cancer has modest effects on survival and is not curative. Although Taxol is one of a few chemotherapeutic agents that have some activity against

**Figure 4.** Evaluation of combination effect of anti-stathmin adenovirus and different chemotherapeutic agents. The Chou and Talalay CI method was used to evaluate the therapeutic interactions between anti-stathmin adenovirus and different chemotherapeutic agents. The Fa-CI plots were constructed using the CalcuSyn software. **A**, Fa-CI plot represents the CI values and the Fa at different concentrations of Taxol (1–6 nmol/L) in cells infected with the anti-stathmin adenovirus. **B**, Fa-CI plot represents the CI values and the Fa at different concentrations of etoposide (0.25–2  $\mu$ mol/L) in cells infected with the anti-stathmin adenovirus. **C**, Fa-CI plot represents the CI values and the Fa at different concentrations of Adriamycin (1–10 nmol/L) in cells infected with the anti-stathmin adenovirus. **D**, Fa-CI plot represents the CI values and the Fa at different concentrations of 5-FU (0.5–5  $\mu$ mol/L) in cells infected with the anti-stathmin adenovirus. *Dashed line*, additive effect of the combination of anti-stathmin adenovirus and the different drugs is represented at CI = 1. A CI of <1 denotes a synergistic interaction, a CI of  $\sim 1$  denotes an additive interaction, and a CI of >1 indicates an antagonistic interaction.



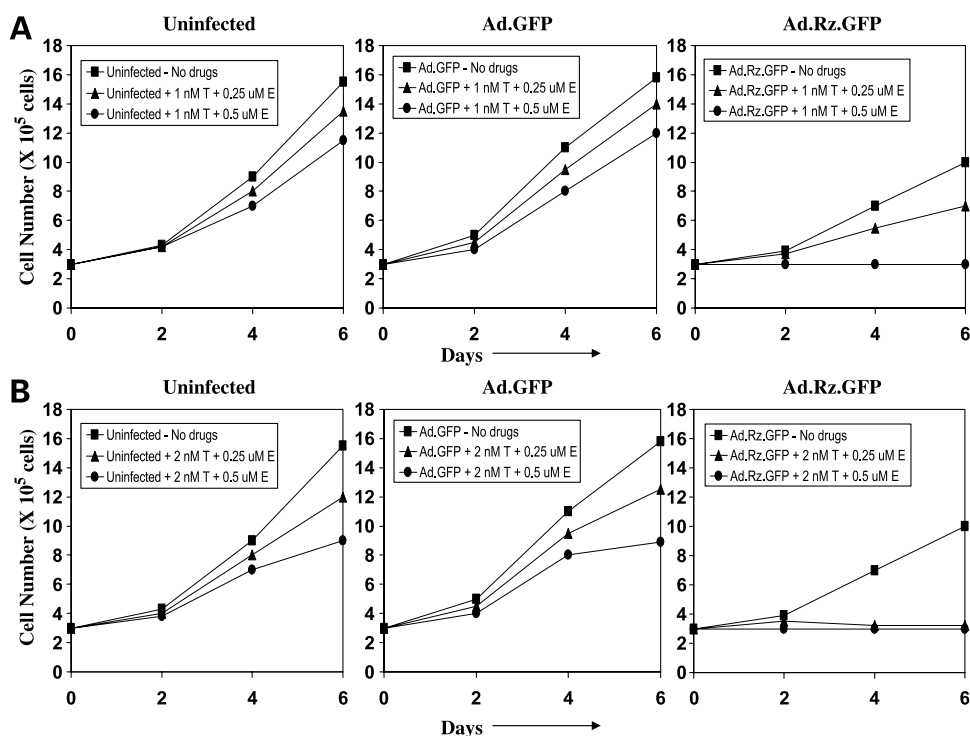


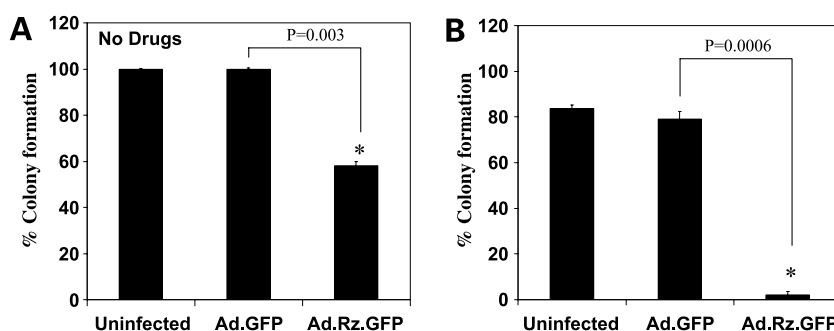
**Figure 5.** Effects of triple combination of anti-stathmin adenovirus, Taxol, and etoposide on the rate of proliferation of LNCaP cells. **A**, growth curves of uninfected cells and cells infected with either control Ad.GFP or Ad.Rz.GFP adenoviruses in the presence and absence of either 1 nmol/L Taxol (T) and 0.25  $\mu$ mol/L etoposide (E) or 1 nmol/L Taxol and 0.5  $\mu$ mol/L etoposide. **B**, growth curves of uninfected cells and cells infected with either control Ad.GFP or Ad.Rz.GFP adenoviruses in the presence and absence of either 2 nmol/L Taxol and 0.25  $\mu$ mol/L etoposide or 2 nmol/L Taxol and 0.5  $\mu$ mol/L etoposide. Points, mean of triplicate alternate day cell counts.

prostate cancer cells *in vitro*, the results of clinical studies in which Taxol was used as a single agent in prostate cancer have been generally disappointing (23, 24). Its clinical use is further reduced due to toxicity associated with its long-term administration at high doses. Thus, the mitotic spindle and the strategies that target mitosis may provide an attractive therapeutic strategy for advanced prostate cancer.

Stathmin may provide an excellent molecular target for prostate cancer therapy (12, 17). We had previously described the design and testing of several anti-stathmin hammerhead ribozymes that cleave stathmin mRNA catalytically (16). More recently, we incorporated these ribozymes into adenoviral gene transfer vectors for targeting stathmin in prostate cancer cells (17). Our studies showed that the anti-stathmin adenoviruses can suppress the malignant phenotype of prostate cancer cells (17). In this report, we examined the hypothesis that an anti-stathmin ribozyme may be of greater therapeutic benefit if combined with chemotherapeutic agents, especially ones that target the mitotic spindle. Thus, we evaluated the therapeutic interactions between an anti-stathmin ribozyme and four different chemotherapeutic agents in assays of proliferation, clonogenicity, and apoptosis in human prostate cancer cells. We examined the effects of combination of anti-stathmin adenovirus with a microtubule-interfering drug (Taxol), a topoisomerase inhibitor (etoposide), an antimetabolite (5-FU), and an anthracycline (Adriamycin). Although the anti-stathmin ribozyme chemosensitized LNCaP cells to all four chemotherapeutic agents, the therapeutic interactions with the different agents were significantly different. In all three assays,

exposure of Ad.Rz.GFP-infected cells to either Taxol or etoposide resulted in striking growth-inhibitory effects, marked inhibition of clonogenic potential, and profound induction of apoptosis. These observations are of considerable clinical interest because complete inhibition of growth could be achieved at concentrations that resulted in <50% inhibition when these chemotherapeutic agents were used as single agents. Just as importantly, profound inhibitory effects were seen at a relatively low MOI of the anti-stathmin adenovirus and at subtherapeutic concentrations of the drugs. In comparison, although exposure of the same cells to 5-FU or Adriamycin potentiated the growth-inhibitory effects of the anti-stathmin ribozyme, the LNCaP cells continued to proliferate. When these interactions were analyzed further by the method of Chou and Talalay, these interactions between anti-stathmin therapy with Taxol or etoposide were clearly synergistic. In contrast, the interaction of 5-FU or Adriamycin with stathmin inhibition was additive. These observations are particularly relevant because prostate cancer is more sensitive to Taxol and etoposide than to 5-FU and Adriamycin. Although most of the cells were infected by the recombinant adenoviruses in the experiments described, we cannot rule out the existence of bystander effects. As seen in Figs. 2 and 8, a small fraction of cells were observed to be GFP negative and were still TUNEL positive (<5%), which is compatible with a bystander effect. Alternatively, it is also possible that the small fraction of GFP-negative cells may have been transduced by very low copy of the virus. Consequently, they may have seemed uninfected by flow cytometry but were phenotypically affected by stathmin inhibition.

**Figure 6.** Effects of triple combination of anti-stathmin adenovirus, Taxol, and etoposide on the clonogenic potential of LNCaP cells. **A**, clonogenicity of uninfected, control Ad.GFP-infected, and Ad.Rz.GFP-infected cells at baseline in the absence of Taxol and etoposide. **B**, clonogenicity of uninfected, control Ad.GFP-infected, and Ad.Rz.GFP-infected cells in the presence of noninhibitory concentrations of Taxol (1 nmol/L) and etoposide (0.5  $\mu$ mol/L). Columns, mean of three different experiments; bars, SD. Statistical significance was determined using Student's *t* test. Asterisks, statistically significant inhibition of clonogenicity.



Because both Taxol and stathmin inhibition interfere with the regulation of the microtubules that make up the mitotic spindle, it is not surprising that the combination of the two interventions would result in a synergistic interaction. These findings are consistent with our previous study that showed synergistic inhibition of growth of K562 leukemic cells on stathmin inhibition and Taxol exposure (25). Nonetheless, the exact molecular mechanism that is responsible for the observed synergistic interaction between stathmin inhibition and Taxol is not clear. Numerous lines of evidence have shown that a deficiency in stathmin decreases the rate of catastrophes and sequestration of tubulin molecules, thereby shifting the equilibrium between the polymerized and unpolymerized tubulin in

favor of polymerized tubulin (1, 3, 26, 27). Taxol, on the other hand, stabilizes microtubules by binding to polymerized tubulin (28). Hence, when stathmin-inhibited cells are exposed to Taxol, the cells will have difficulty depolymerizing the microtubules due to stathmin deficiency and the polymerized microtubules will be further stabilized by Taxol binding. This may explain, at least in part, the observed synergy between stathmin inhibition and Taxol exposure.

As we had previously seen with Taxol exposure (25), exposure of cells to etoposide also arrests cells in the  $G_2$ -M phases of the cell cycle, eventually leading to apoptotic cell death (data not shown). However, unlike Taxol, microtubule staining of etoposide-treated LNCaP cells revealed

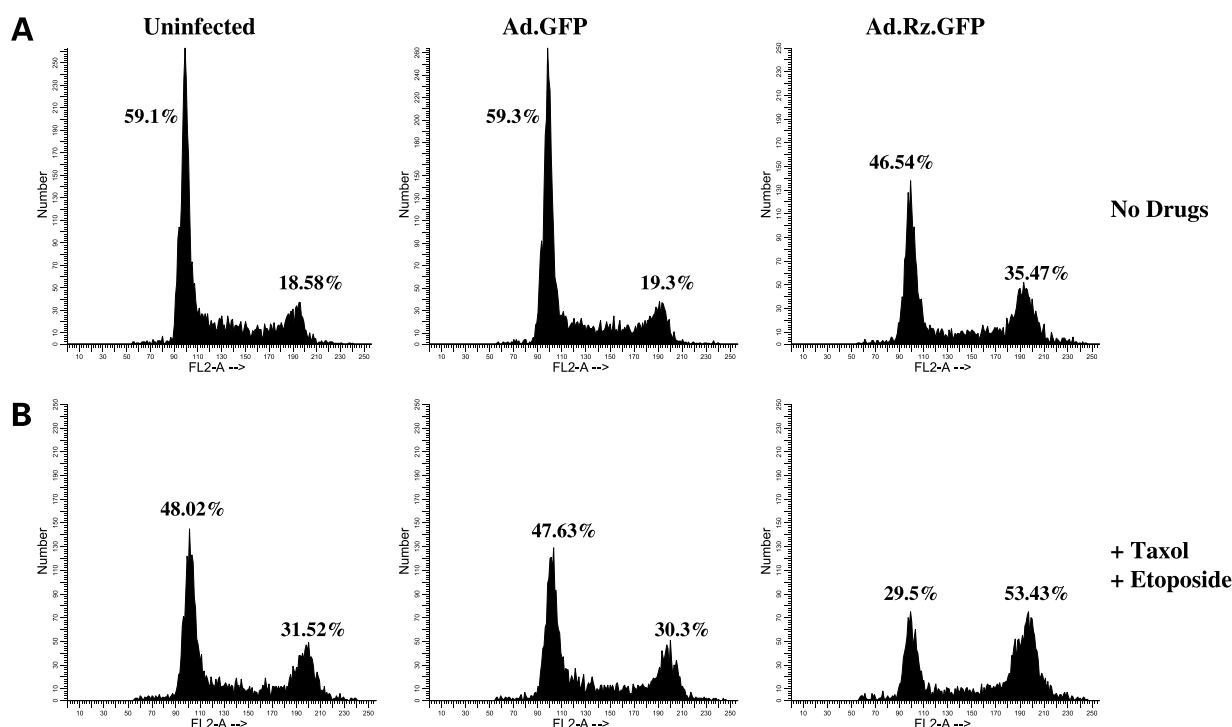


**Figure 7.** Effects of triple combination of anti-stathmin adenovirus, Taxol, and etoposide on the cell cycle distribution of LNCaP cells. **A**, DNA histograms of uninfected cells, cells infected with the control Ad.GFP, and cells infected with Ad.Rz.GFP adenovirus in the absence of drug exposure. **B**, DNA histograms of uninfected cells, cells infected with the control Ad.GFP, and cells infected with Ad.Rz.GFP adenovirus after 48 h of exposure to 1 nmol/L Taxol and 0.5  $\mu$ mol/L etoposide.

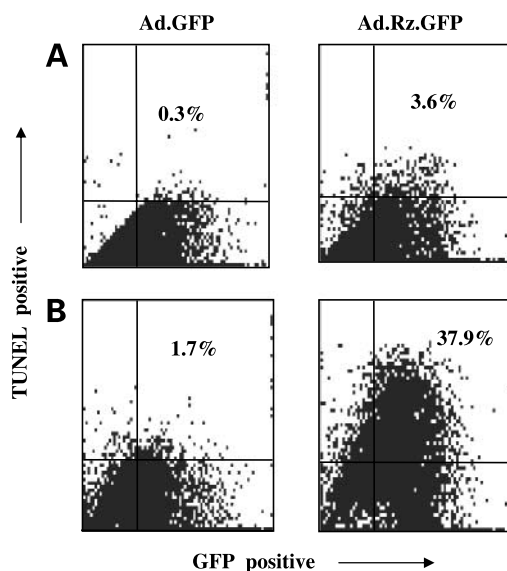


**Figure 8.** Effects of triple combination of anti-stathmin adenovirus, Taxol, and etoposide on apoptosis in LNCaP cells. **A**, dot plot showing the fraction of TUNEL positivity in Ad.GFP- and Ad.Rz.GFP-infected cells in the absence of Taxol and etoposide. **B**, dot plot showing the fraction of TUNEL positivity in Ad.GFP- and Ad.Rz.GFP-infected cells in the presence of noninhibitory concentrations of Taxol (1 nmol/L) and etoposide (0.5  $\mu$ mol/L). The experiment is a representative of three independent experiments.

very rare mitotic figures (data not shown). This suggests that exposure to etoposide blocks cells in the  $G_2$  phase of the cell cycle. These observations agree with the studies of Lock and Ross (29) and Lock (30) who showed that exposure of Chinese hamster ovary cells to etoposide results in a decline in the mitotic index and the arrest of cells in late  $G_2$  phase. They also showed that the etoposide-induced  $G_2$  arrest results from the rapid inhibition of the activity of p34<sup>cdc2</sup>, a protein kinase that is critical for the transition from the  $G_2$  phase into mitosis in eukaryotic cells (29, 30). p34<sup>cdc2</sup> kinase is known to phosphorylate a variety of cellular proteins, including Rb and p53, in a cell cycle-dependent manner (31, 32). Previous studies from our own laboratory had shown a cell cycle-dependent increase in the level of phosphorylation of stathmin in the  $G_2$ -M phases that is mediated by p34<sup>cdc2</sup> kinase (6). When stathmin is phosphorylated by p34<sup>cdc2</sup> kinase as cells enter mitosis, its microtubule-depolymerizing activity is lost, tubulin is polymerized, and the mitotic spindle is formed (2). In subsequent studies, we had also shown that dephosphorylation of stathmin late in mitosis is necessary for spindle disassembly and the exit from mitosis (3, 4). Thus, in cells exposed to etoposide in which stathmin is inhibited, the cells might have difficulty entering mitosis due to inhibition of p34<sup>cdc2</sup> kinase and difficulty exiting mitosis due to stathmin deficiency.

We believe that the effects of the triple combination of anti-stathmin therapy with Taxol and etoposide at low noninhibitory concentrations may be important for the design of effective therapies in the future. In all three

assays, the observed effects were much greater than the effects of ribozyme with Taxol or ribozyme with etoposide. Although synergistic interactions were observed when anti-stathmin therapy was combined with either Taxol or etoposide at subtherapeutic concentrations, the triple combination resulted in complete inhibition of growth and clonogenicity at low noninhibitory concentrations of the drugs. We hypothesize that, when the prostate cancer cells in which stathmin is inhibited are exposed to Taxol and etoposide simultaneously, cells will have difficulty entering mitosis, depolymerizing their spindles, and exiting mitosis. This hypothesis is supported by a more profound  $G_2$ -M arrest in cells exposed to Taxol and etoposide in the presence of stathmin inhibition than in the absence of stathmin inhibition (Fig. 7). Thus, anti-stathmin ribozyme can markedly enhance the effects of low noninhibitory (and probably nontoxic) concentrations of Taxol and etoposide and may lead to profound inhibition of tumor growth and marked induction of apoptosis. Because Taxol and etoposide are two of the most active chemotherapeutic agents in prostate cancer, combination of these agents with stathmin inhibition may provide a superior form of combination therapy that would also avoid toxicities associated with the use of multiple chemotherapeutic agents at their maximally tolerated doses.

## References

1. Belmont LD, Mitchison TJ. Identification of a protein that interacts with tubulin dimers and increases the catastrophe rate of microtubules. *Cell* 1996;84:623–31.
2. Marklund U, Larsson N, Gradin H, Brattsand G, Gullberg M. Oncoprotein 18 is a phosphorylation-responsive regulator of microtubule dynamics. *EMBO J* 1996;15:5290–8.
3. Mistry SJ, Atweh GF. Stathmin inhibition enhances okadaic acid-induced mitotic arrest: a potential role for stathmin in mitotic exit. *J Biol Chem* 2001;276:31209–15.
4. Mistry SJ, Li HC, Atweh GF. Role for protein phosphatases in the cell-cycle-regulated phosphorylation of stathmin. *Biochem J* 1998;334:23–9.
5. Marklund U, Brattsand G, Shingler V, Gullberg M. Serine 25 of oncoprotein 18 is a major cytosolic target for the mitogen-activated protein kinase. *J Biol Chem* 1993;268:15039–47.
6. Luo XN, Mookerjee B, Ferrari A, Mistry S, Atweh GF. Regulation of phosphoprotein p18 in leukemic cells. Cell cycle regulated phosphorylation by p34cdc2 kinase. *J Biol Chem* 1994;269:10312–8.
7. Larsson N, Melander H, Marklund U, Osterman O, Gullberg M.  $G_2$ /M transition requires multisite phosphorylation of oncoprotein 18 by two distinct protein kinase systems. *J Biol Chem* 1995;270:14175–83.
8. Horwitz SB, Shen HJ, He L, et al. The microtubule-destabilizing activity of metablastin (p19) is controlled by phosphorylation. *J Biol Chem* 1997;272:8129–32.
9. Hanash SM, Strahler JR, Kuick R, Chu EHY, Nichols D. Identification of a polypeptide associated with the malignant phenotype in acute leukemia. *J Biol Chem* 1988;263:12813–5.
10. Roos G, Brattsand G, Landberg G, Marklund U, Gullberg M. Expression of oncoprotein 18 in human leukemias and lymphomas. *Leukemia* 1993;7:1538–46.
11. Brattsand G. Correlation of oncoprotein 18/stathmin expression in human breast cancer with established prognostic factors. *Br J Cancer* 2000;83:311–8.
12. Friedrich B, Gronberg H, Landstrom M, Gullberg M, Bergh A. Differentiation-stage specific expression of oncoprotein 18 in human and rat prostatic adenocarcinoma. *Prostate* 1995;27:102–9.

13. Mistry S, Atweh GF. Role of stathmin in the regulation of the mitotic spindle: potential applications in cancer therapy. *Mt Sinai J Med* 2002;69:299–304.
14. Mistry SJ, Atweh GF. Stathmin expression in immortalized and oncogene transformed cells. *Anticancer Res* 1999;19:573–8.
15. Jeha S, Luo XN, Beran M, Kantarjian H, Atweh GF. Antisense RNA inhibition of phosphoprotein p18 expression abrogates the transformed phenotype of leukemic cells. *Cancer Res* 1996;56:1445–50.
16. Mistry SJ, Benham CJ, Atweh GF. Development of ribozymes that target stathmin, a major regulator of the mitotic spindle. *Antisense Nucleic Acid Drug Dev* 2001;11:41–9.
17. Mistry SJ, Bank A, Atweh GF. Targeting stathmin in prostate cancer. *Mol Cancer Ther* 2005;4:1821–9.
18. Gao M, Ossowski L, Ferrari AC. Activation of Rb and decline in androgen receptor protein precede retinoic acid-induced apoptosis in androgen-dependent LNCaP cells and their androgen-independent derivative. *J Cell Physiol* 1999;179:336–46.
19. Graham F, Prevec L. Methods for construction of adenovirus vectors. *Mol Biotechnol* 1995;3:207–20.
20. Chou TC, Talalay P. Quantitative analysis of dose effect relationships: the combined effects of multiple drugs or enzyme inhibitors. *Adv Enzyme Regul* 1984;22:27–55.
21. Freedman VH, Shin SI. Cellular tumorigenicity in nude mice correlates with cell growth in semi-solid medium. *Cell* 1974;3:355–9.
22. Shin SI, Freedman VH, Risser R, Pollack R. Tumorigenicity of virus-transformed cells in nude mice is correlated specifically with anchorage independent growth *in vitro*. *Proc Natl Acad Sci U S A* 1975;72:4435–9.
23. Kang MH, Figg WD, Dahut W. Taxanes in hormone-refractory prostate cancer. *Cancer Pract* 1999;7:270–2.
24. Roth BJ, Yeap BY, Wilding G, Kasimis B, McLeod D, Loehrer PJ. Taxol in advanced, hormone-refractory carcinoma of the prostate. A phase II trial of the Eastern Cooperative Oncology Group. *Cancer* 1993;72:2457–60.
25. Iancu C, Mistry SJ, Arkin S, Atweh GF. Taxol and anti-stathmin therapy: a synergistic combination that targets the mitotic spindle. *Cancer Res* 2000;60:3537–41.
26. Howell B, Deacon H, Cassimeris L. Decreasing oncoprotein 18/stathmin levels reduces microtubule catastrophes and increases microtubule polymer *in vivo*. *J Cell Sci* 1999;112:3713–22.
27. Jourdain L, Curmi P, Sobel A, Dominique P, Carlier M-F. Stathmin: a tubulin-sequestering protein which forms a ternary T2S complex with two tubulin molecules. *Biochemistry* 1997;36:10817–21.
28. Parness J, Horwitz SB. Taxol binds to polymerized tubulin *in vitro*. *J Biol Chem* 1981;91:479–87.
29. Lock RB, Ross WE. Inhibition of p34cdc2 kinase activity by etoposide or irradiation as a mechanism of G<sub>2</sub> arrest in Chinese hamster ovary cells. *Cancer Res* 1990;50:3761–6.
30. Lock RB. Inhibition of p34cdc2 kinase activation, p34cdc2 tyrosine dephosphorylation, and mitotic progression in Chinese hamster ovary cells exposed to etoposide. *Cancer Res* 1992;52:1817–22.
31. Lin B-Y, Gruenwald SD, Maria A, Lee W-H, Wang JY. Retinoblastoma cancer suppressor gene product is a substrate of the cell cycle regulator cdc2 kinase. *EMBO J* 1991;10:857–64.
32. Sturzbecher HW, Maineta T, Chumakov P, et al. p53 interacts with p34cdc2 kinase in mammalian cells: implications for cell cycle control and oncogenesis. *Oncogene* 1990;5:795–801.